



Deposited via The University of Leeds.

White Rose Research Online URL for this paper:

<https://eprints.whiterose.ac.uk/id/eprint/87261/>

Version: Accepted Version

Article:

Lord, RM, Hebden, AJ, Pask, CM et al. (2015) Hypoxia-Sensitive Metal β -Ketoiminato Complexes Showing Induced Single-Strand DNA Breaks and Cancer Cell Death by Apoptosis. *Journal of Medicinal Chemistry*, 58 (12). pp. 4940-4953. ISSN: 0022-2623

<https://doi.org/10.1021/acs.jmedchem.5b00455>

(c) 2015, American Chemical Society. This document is the Accepted Manuscript version of a Published Work that appeared in final form in *Journal of Medicinal Chemistry*, copyright © American Chemical Society after peer review and technical editing by the publisher. To access the final edited and published work see <https://doi.org/10.1021/acs.jmedchem.5b00455>

Reuse

Items deposited in White Rose Research Online are protected by copyright, with all rights reserved unless indicated otherwise. They may be downloaded and/or printed for private study, or other acts as permitted by national copyright laws. The publisher or other rights holders may allow further reproduction and re-use of the full text version. This is indicated by the licence information on the White Rose Research Online record for the item.

Takedown

If you consider content in White Rose Research Online to be in breach of UK law, please notify us by emailing eprints@whiterose.ac.uk including the URL of the record and the reason for the withdrawal request.

Hypoxia Sensitive Metal β -Ketoiminato Complexes Showing Induced Single Strand DNA Breaks and Cancer Cell Death by Apoptosis

Rianne M. Lord,^a Andrew J. Hebden,^a Christopher M. Pask,^a Imogen R. Henderson,^a Stephanie J. Lucas,^a Simon J. Allison,^b Samantha L. Shepherd,^c Roger M. Phillips,^c and Patrick C. McGowan.^{a*}

^a School of Chemistry, University of Leeds, Leeds, UK, LS2 9JT. Email: p.c.mcgowan@leeds.ac.uk, Tel: +44(0)113 3436404

^b Institute of Cancer Therapeutics, University of Bradford, Bradford, UK, BD7 1DP

^c Department of Pharmacy, School of Applied Sciences, University of Huddersfield, Huddersfield, HD1 3DH

ABSTRACT: A series of ruthenium and iridium complexes have been synthesised and characterised with 20 novel crystal structures discussed. The library of β -ketoiminato complexes has been shown to be active against MCF-7 (human breast carcinoma), HT-29 (human colon carcinoma), A2780 (human ovarian carcinoma) and A2780cis (cisplatin resistant human ovarian carcinoma) cell lines, with selected complexes being more than three times as active as cisplatin against the A2780cis cell line. Complexes have also been shown to be highly active under hypoxic conditions, with the activities of some complexes increasing with a decrease in O₂ concentration. The enzyme thioredoxin reductase is over-expressed in cancer cells and complexes reported herein have the advantage of inhibiting this enzyme, with IC₅₀ values measured in the nanomolar range. The anti-cancer activity of these complexes was further investigated to determine whether activity is due to effects on cellular growth or cell survival. The complexes were found to induce significant cancer cell death by apoptosis with levels induced correlating closely with activity in chemosensitivity studies. As a possible cause of cell death, the ability of the complexes to induce damage to cellular DNA was also assessed. The complexes failed to induce double strand DNA break or DNA crosslinking but induced significant levels of single DNA strand breaks indicating a different mechanism of action to cisplatin.

Introduction

Ruthenium has become one of the most popular metals used in drug development due to the metal's easily accessible oxidation states, stability in air and the relative ease of synthesis of organometallic and coordination complexes. Most importantly ruthenium is thought to have slow *in vivo* ligand exchange and higher selectivity towards cancer cells leading to lower toxicity.¹⁻⁴ The discovery of organometallic ruthenium complexes first began with the library of $[(\eta^6\text{-arene})\text{Ru(II)}(\text{en})\text{X}]^+$ (X = halide, en = ethylenediamine) complexes synthesised by Sheldrick *et al.*⁵⁻⁷ The effect of the ligand was later explored by Sadler *et al.* substituting the neutral (N,N) ethylenediamine ligand for an anionic (O,O) β -diketonato ligand, showing a significant increase in cytotoxicity of the complexes.⁸ In collaboration with Sadler, McGowan *et al.* first synthesised picolinamide Ru(II) and Os(II) arene complexes due to their relevance to previously reported metal ion-peptide chemistry⁹⁻¹¹ and the possibility of different binding modes, through either a monoanionic (N,N) or a neutral (N,O) form. Studies showed that the more cytotoxic (N,N) complexes undergo rapid hydrolysis and bind preferentially to guanine, whereas switching the binding mode to (N,O) slows the rate of hydrolysis and switches off the activity.^{12,13} McGowan *et al.* also

synthesised ruthenium and iridium complexes incorporating either a picolinamide (N,N), β -ketoiminato (N,O) or a naphthoquinone (O,O) ligand and compared the effects of these substitutions upon cytotoxicity. The IC₅₀ values obtained for both HT-29 and MCF-7 cancer cell lines suggest that the binding mode is a critical determinant of complex activity. The lowest IC₅₀ values were observed for the β -ketoiminato (N,O) complexes for both ruthenium and iridium and anti-cancer activity followed the general trend (N,O) > (O,O) > (N,N).¹⁴

Herein we report the synthesis and characterisation of a new series of (N,O) and (O,O) complexes and analysis of their biological effects, gaining an understanding of their biological mechanisms. We report on the cytotoxic potential of our library of novel complexes, with potent cancer cell cytotoxicity observed, particular against the cisplatin resistant ovarian cell line (A2780cis). As many tumours have a significant hypoxic fraction and hypoxic tumour cells are typically resistant to standard chemotherapy and radiotherapy,¹⁵⁻¹⁷ IC₅₀ values were also obtained for cells grown under low oxygen conditions. This enabled us to evaluate the potential of these complexes for targeting tumour cells that reside in a hypoxic microenvironment and which are a common cause of chemoresistance and tumour recurrence. Further

mechanistic studies have been undertaken to assess whether the anti-cancer activity of the novel complexes is due to effects upon cellular growth and proliferation or due to effects upon cell survival. The complexes were tested against HT-29 and A2780 cells at varying concentrations and effects on cell phenotype determined. Cell images were recorded under phase contrast microscopy at various time-points and levels of cell death by apoptosis and necrosis were quantified. Studies have also been carried out to assess the possibility of thioredoxin reductase (Trx-R) inhibition, using UVvis spectroscopy to monitor Trx-R activity following incubation of Trx-R enzyme with varying concentrations of our complexes. Finally, more detailed mechanistic studies have been carried out for possible damage to cellular DNA, given the ability of previous (*N,N*) complexes to bind guanine.^{12,13} The complexes have been assessed for double strand DNA breaks (DSB), DNA cross-linking and single strand DNA breaks (SSB) using the Comet assay to quantify levels of different types of DNA damage in single cells, in order to gain structure activity relationships.

Selective modifications were made within the library of complexes to gain an understanding of the characteristics needed for high *in vitro* cytotoxicity (Figure 1) with the following variables being assessed:

- removal of steric bulk, reducing the size of the ligand
- changing the binding mode of the ligand – (*N,O*) versus (*O,O*)
- changing the arene substituent – *p*-cymene or Cp*
- altering the metal centre – ruthenium versus iridium

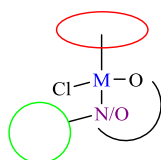


Figure 1 Modifications of the ‘piano stool’ complexes

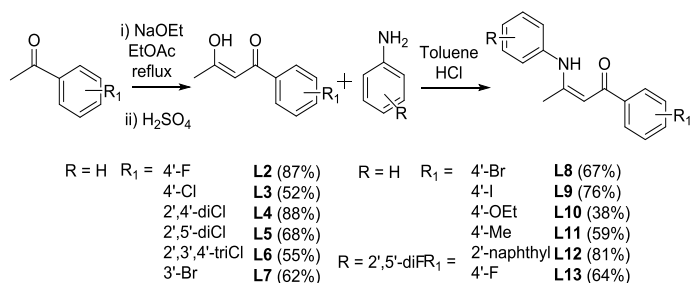
Results and discussion

Synthesis and Characterisation

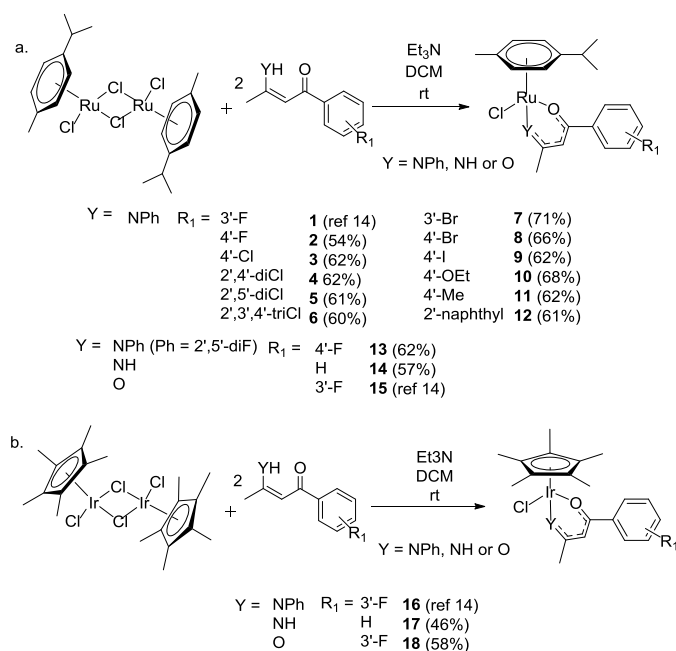
The β -ketoenamine ligands **L2-L13** were synthesised according to Scheme 1. Ligand **L14** has previously been reported by Roshchupkina *et al.*¹⁸ The corresponding β -diketonate ligands were prepared¹⁹ and dissolved with stirring in toluene, followed by addition of excess aniline and hydrochloric acid.^{20,21} Ligands were obtained as analytically pure compounds from solutions of hot ethanol in yields of 38-88% and characterised by ¹H NMR spectroscopy, ¹³C{¹H} NMR spectroscopy, mass spectrometry and microanalysis. Ligands **L3-6**, **8** and **11** were also characterised by single crystal X-ray crystallography.

The half-sandwich β -ketoiminato and β -diketonato complexes were synthesised according to Scheme 2. One

equivalent of either [*p*-cymRuCl₂]₂ (Scheme 2a) or [Cp*IrCl₂]₂ (Scheme 2b) was stirred with two equivalents of the functionalised ligand and two equivalents of triethylamine in dichloromethane. Complexes **1-18** were isolated as analytically pure complexes from methanolic solutions in yields 46-71% and have been characterised by ¹H NMR spectroscopy, ¹³C{¹H} NMR spectroscopy, mass spectrometry and microanalysis.¹⁴ Complexes **2**, **4-14** and **17-18** were also characterised by single crystal X-ray crystallography.



Scheme 1 General synthetic route for the β -ketoenamine ligands



Scheme 2 General synthetic pathway for: a. Ru(II) complexes and b. Ir(III) complexes

X-ray crystallographic data has been analysed for the novel β -ketoenamine ligands **L3-6**, **8** and **11**, and single crystals were obtained by slow evaporation from hot ethanol. All angles around the central atoms are between 118-125° (see Tables S1-2, SI), showing this section of the ligand is planar, with the atoms held together by an intramolecular hydrogen bonding interaction between N-H...O (Figure 2) which is a feature in all crystal structures.

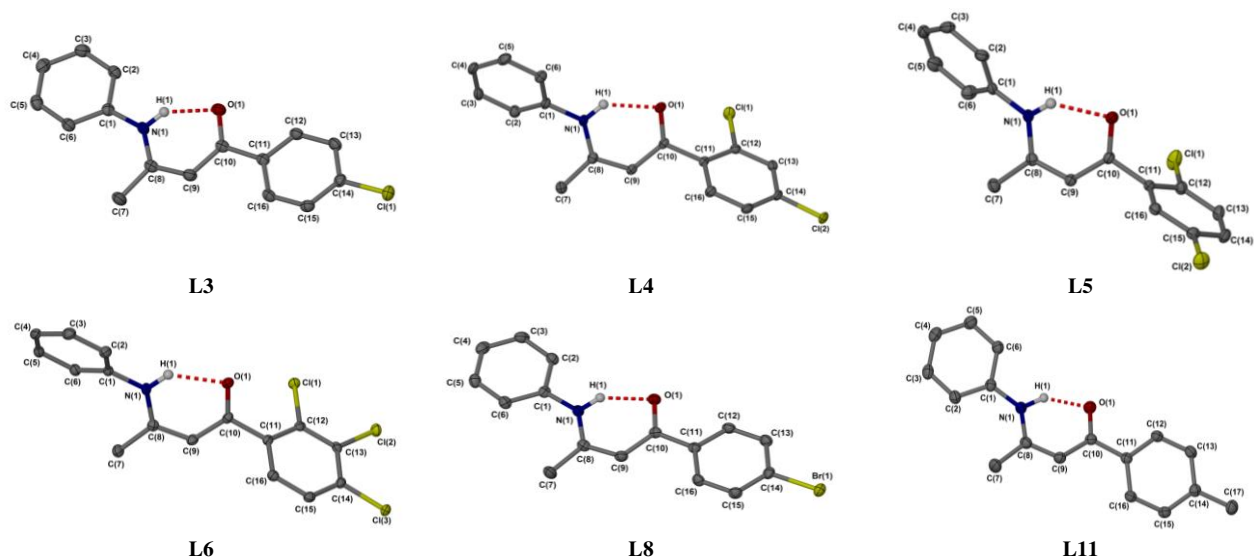


Figure 2 Molecular structures for ligands L3-6, 8 and 11. Hydrogen atoms omitted for clarity. Displacement ellipsoids are at the 50% probability level

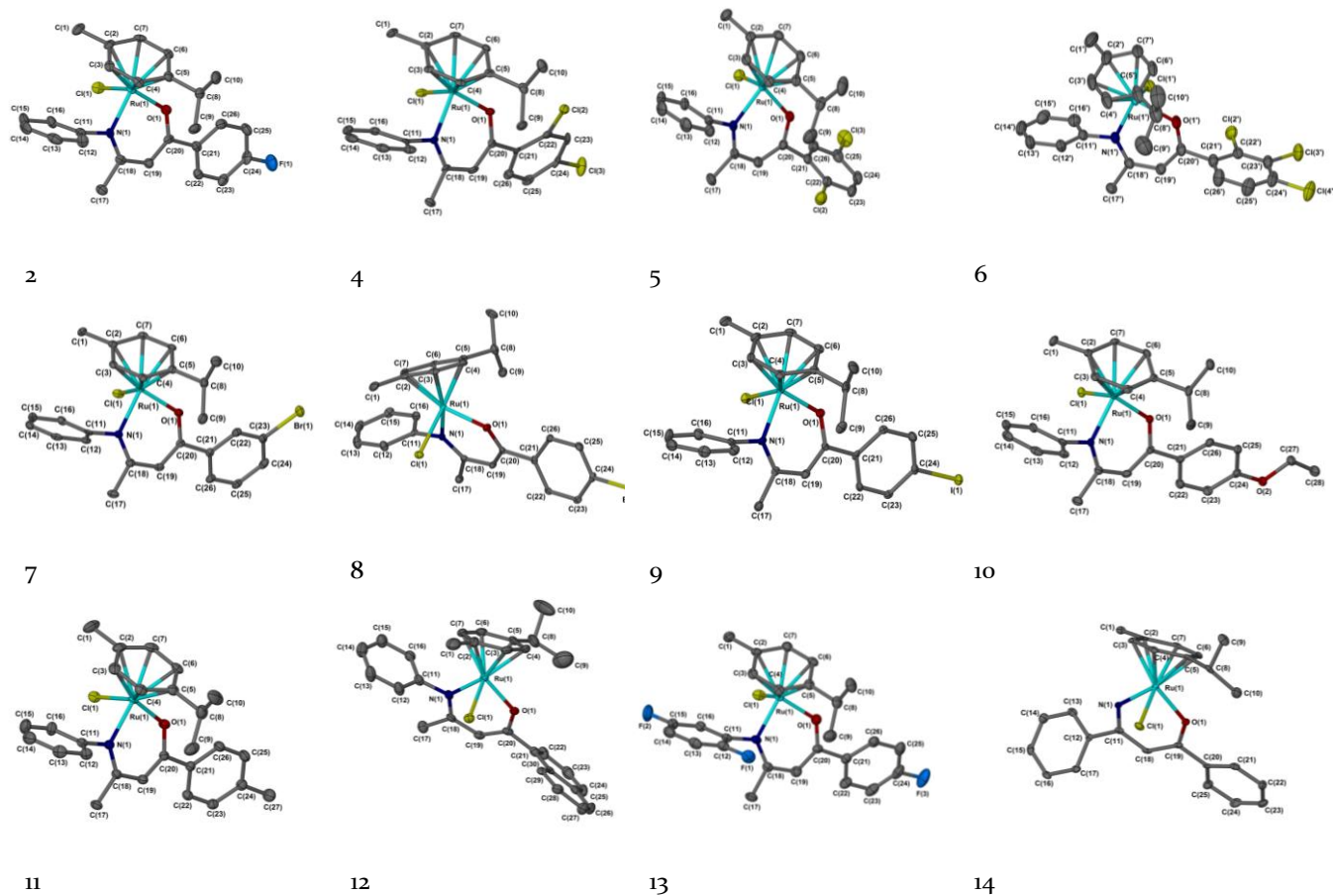


Figure 3a Molecular structures for complexes 2 and 4-14. Hydrogen atoms omitted for clarity. Displacement ellipsoids are at the 50% probability level

X-ray crystallographic data has been analysed for complexes **2**, **4-14**, **17** and **18**, and all single crystals were obtained using slow evaporation from a methanolic solution, appearing as orange/ red (ruthenium) or yellow (iridium) single crystals. Solutions were performed in a monoclinic *Cc* (**4** and **7**) or *P2₁/c* (**14**), triclinic *P* $\bar{1}$ (**2**, **5**, **6**, **8-13** and **17**), or orthorhombic *P2₁2₁2₁* (**18**) space groups. All of the angles around the metal centre show the geometry expected for *pseudo* octahedral compounds which is common for half-sandwich “piano-stool” structures (see **Tables S3-4**, *SI*). The angles between the metal and bidentate ligands are in the range 83-90°, with the remaining three coordination sites occupied by the *p*-cymene or Cp* ligand and the angles observed for their centroids to the chloride or bidentate ligand ranges between 124-133°. Molecular structures for complexes **2**, **4-14**, **17** and **18** are shown in **Figure 3a** and **3b**, with displacement ellipsoids placed at the 50% probability level and hydrogen atoms omitted for clarity.

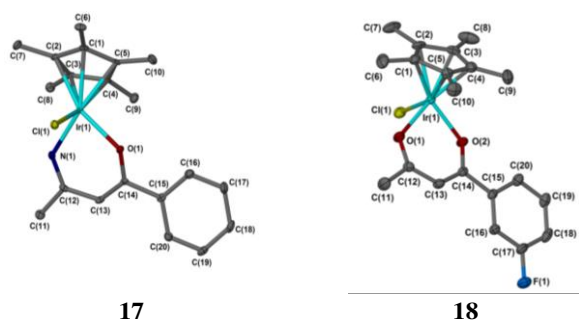


Figure 3b Molecular structures for iridium(III) complexes **17** and **18**. Hydrogen atoms omitted for clarity. Displacement ellipsoids are at the 50% probability level

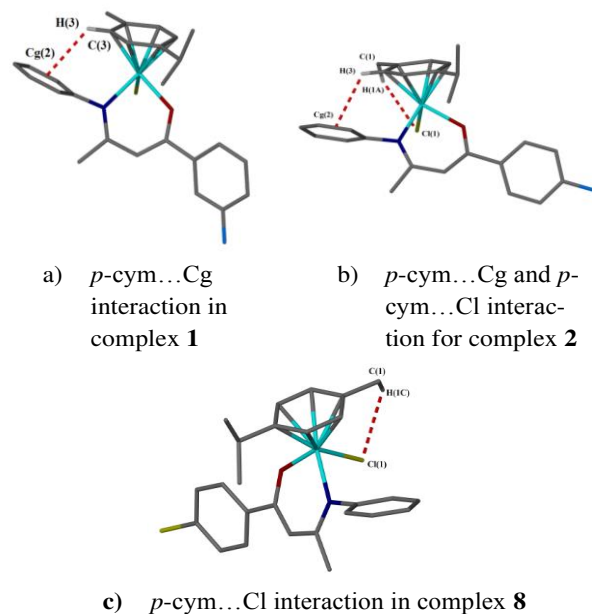


Figure 4 Intramolecular interactions for a) complex **1**, b) complex **2** and c) complex **8**

The ¹H NMR spectra for the ruthenium β -ketoiminato complexes show a significant upfield shift of 1.3-1.6 ppm for one of the *p*-cymene hydrogens. Analysis of the X-ray structure shows one of these hydrogens undergoes intramolecular T-stacking interactions with the aniline ring at D...A distances between 3.33-3.62 Å (**Figure 4**). This type of interaction has previously been reported with a library of complexes of the type [areneRuCl(XY)] (where XY = *N,O* ligand) synthesised by Dyson *et al.*, in which it was noted these complexes can exist as two conformers, with variable temperature NMR studies showing the presence of both conformers at lower temperatures.²² Interactions are also seen between the *p*-cymene hydrogen and the ancillary chloride ligand with D...A distances of 3.37-3.34 Å (**Figure 4**).

Cell Line Chemosensitivity Studies

In order to gain information about the structure-activity relationships of the different complexes, chemosensitivity studies were performed and IC₅₀ values were determined for HT-29, MCF-7, A2780 and A2780cis cancer cell lines exposed to each of complexes **1-18** or to cisplatin (**Table 1** and **Figure S2**). The results show that the ruthenium β -ketoiminato complexes are all cytotoxic towards the cancer cell lines tested, with particular activity against both A2780 and A2780cis cell lines. Complex **1** was the most active complex against all four cancer cell lines, with the lowest IC₅₀ value for MCF-7 of 1.9 ± 0.1 μM (cisplatin 0.98 ± 0.09 μM), and significant activity against the cisplatin-resistance cell line A2780cis in which it was ~3-fold more active than cisplatin (3.13 ± 0.09 μM versus 10.5 ± 0.2 μM). This suggests that the mechanism of action and resistance of these complexes is different from cisplatin and raises the possibility that some of these complexes could potentially be used to treat cancer which has become resistant to cisplatin. This library shows that complexes **1-7**, which have electron withdrawing substituents, are the most potent against all tested cell lines. While introduction of electron donating groups or sterically bulky groups usually leads to a slight decrease in activity (complexes **11**, **12**, **14**, **16** and **17**). However, on comparison of substituents in the *para* position, when a methyl substituent was introduced (complex **11**), anti-cancer activity increased in comparison to the *para* electron withdrawing substituents and this complex was the most active *para* complex against MCF-7 cells, with an IC₅₀ value of 2.1 ± 0.1 μM (cisplatin 1.07 ± 0.10 μM). Control experiments were also performed to investigate whether the ligands alone possess any cytotoxic activity *in vitro*. Ligands **L2-4** and **L7** were tested against HT-29 cancer cells and all were considered to be inactive with IC₅₀ values greater than the tested threshold (>250 μM) (**Table 1**).

Table 1 IC₅₀ values for cisplatin and complexes 1-18 against HT-29, MCF-7, A2780, A2780cis and ARPE-19 cell lines. The values in parenthesis represent the IC₅₀ values for the ARPE-19 cells divided by IC₅₀ values for individual cancer cells (values greater than 1 indicate selectivity for cancer cells over the non-cancer ARPE-19 cells).

Complex	HT-29 IC ₅₀ (μM) ± SD	MCF-7 IC ₅₀ (μM) ± SD	A2780 IC ₅₀ (μM) ± SD	A2780cis IC ₅₀ (μM) ± SD	ARPE-19 IC ₅₀ (μM) ± SD
Cisplatin	2.40 ± 0.10 (2.49)	1.09 ± 0.08 (5.47)	0.94 ± 0.04 (6.35)	10.50 ± 0.20 (0.57)	5.97 ± 0.95
1	3.50 ± 0.30 (1.28)	1.90 ± 0.10 (2.36)	2.60 ± 0.08 (1.72)	3.13 ± 0.09 (1.43)	4.48 ± 0.07
2	10.50 ± 0.40	5.07 ± 0.09	2.80 ± 0.10	3.47 ± 0.07	-
3	5.40 ± 0.09	3.00 ± 0.20	1.70 ± 0.10	3.80 ± 0.10	-
4	4.30 ± 0.50	3.22 ± 0.09	2.35 ± 0.04	5.59 ± 0.05	-
5	11.40 ± 0.60	3.50 ± 0.20	2.50 ± 0.10	6.40 ± 0.10	-
6	12.60 ± 0.02	3.27 ± 0.08	2.86 ± 0.04	11.50 ± 0.30	-
7	6.10 ± 0.30 (1.27)	3.55 ± 0.09 (2.18)	2.5 ± 0.2 (3.10)	3.69 ± 0.09 (2.10)	7.76 ± 0.07
8	10.30 ± 0.60 (1.48)	6.20 ± 0.20 (2.47)	2.3 ± 0.2 (6.67)	7.00 ± 0.04 (2.19)	15.33 ± 0.41
9	11.80 ± 0.80 (1.02)	-	-	-	12.00 ± 1.47
10	12.80 ± 0.50	-	-	-	-
11	10.21 ± 0.09 (0.89)	2.90 ± 0.10 (3.16)	2.87 ± 0.05 (3.19)	9.1 ± 0.1 (1.01)	9.17 ± 2.36
12	22.00 ± 2.00 (0.32)	13.00 ± 0.20 (0.55)	-	-	7.17 ± 0.93
13	6.30 ± 0.30 (0.57)	7.20 ± 0.20 (0.50)	1.90 ± 0.10 (1.91)	3.80 ± 0.09 (0.95)	3.62 ± 0.03
14	53.00 ± 1.00 (0.60)	-	56.00 ± 2.00 (0.57)	-	32.03 ± 9.23
15	18.00 ± 2.00 (2.86)	18.40 ± 0.80 (2.80)	19.40 ± 0.80 (2.66)	24.30 ± 0.50 (2.12)	51.55 ± 5.14
16	5.10 ± 0.30	3.40 ± 0.20	5.70 ± 0.10	5.80 ± 0.50	-
17	83.00 ± 3.00	-	-	-	-
18	93.00 ± 7.00 (>1)	51.00 ± 4.00 (>2)	35.00 ± 1.00 (>2.9)	51.00 ± 1.00 (>2)	>100
L2	> 250	-	-	-	-
L3	> 250	-	-	-	-
L4	> 250	-	-	-	-
L7	> 250	-	-	-	-

Selectivity for cancer cells

Comparing the response of tumour cell lines to non-cancer ARPE-19 cells provides a preliminary indication of selectivity. Whilst compounds **9**, **12**, **13** and **14** show no selectivity towards cancer cells (ratio of IC₅₀ values in AREP-19 cells to cancer cells ≤ 1), compounds **1**, **7**, **8**, **11** and **15** showed evidence of selectivity to certain cancer cells (**Table 1**). The magnitude of the selectivity observed in the test compound series was comparable to that obtained for cisplatin with ratio's of IC₅₀ values in ARPE-19 to cancer cells ranging from 6.67 to 1.27 for test compounds and 6.35 to 0.57 for cisplatin (**Table 1**). Compound **8** in particular demonstrated good selectivity against all the cancer cell lines tested with selectivity ranging from 6.67 to 1.48 fold increased chemosensitivity towards cancer cells compared to ARPE-19 non-cancer cells (A2780: 6.67; A2780cis: 2.19; MCF7: 2.47; HT29: 1.48; **Table 1**). These results provide a preliminary indication that some compounds are selectively toxic to cancer cells.

Due to the high *in vitro* activity for complex **1**, complexes **15**, **16** and **18** were synthesised in order to make comparisons between the biological mechanisms on changing both the ligands and metal centres. Complexes **1** and **16** incorporate a 3-fluoro-β-ketoiminato (*N,O*) ligand, whilst complex **15** and **18** incorporate the 3-fluoro-β-diketonato (*O,O*) ligand, on ruthenium and iridium respectively. On comparison of complex **1** (*N,O*) and the β-diketonato complex **15** (*O,O*), changing the binding mode and hence elimination of the aniline ring, dramatically decreased cell line cytotoxicity, with complex **15** being up to 9-fold less active than its (*N,O*) analogue. Also on comparison of two (*N,O*) complexes **1** and **14**, substituting the aniline ring for NH (**14**) showed a 21-fold decrease in activity when compared to **1**. The iridium Cp* β-ketoiminato complex **16** was synthesised and compared to the iridium β-diketonato analogue **18**. As seen with the ruthenium complexes, the (*O,O*) ligand had up to an 18-fold decrease in activity against HT-29. Again on comparison of two (*N,O*) complexes **16** and **17**, the aniline was substituted for NH (**17**) and the activity decreased by 16-fold when compared to complex **16**.

These results indicate that for the complexes tested, the aniline ring is critical for high *in vitro* anti-cancer activity and on elimination of this ring complex activity is substantially diminished, proving that the design of the ligand is essential in drug development.

Influence of Hypoxia

For many solid tumours, a significant proportion of the tumour cells are under conditions of limiting oxygen or hypoxia and the cellular environment is reducing. The hypoxia-inducible factor-1 (HIF-1) is central to the cell's response to hypoxia and under hypoxic conditions it activates a transcriptional program that helps tumour cell adaptation and survival under low oxygen conditions.²³⁻²⁷ Transition metals have the potential to be reduced under hypoxic conditions and these changes in oxidation states could lead to changes in structure, binding mode, cellular drug uptake and metabolism as well cellular mechanism of action and the effectiveness of this. Using complexes **1**, **15**, **16** and **18**, 5-day *in vitro* MTT studies were conducted under hypoxic conditions at both 0.1% and 1.0% O₂ against HT-29 cells, in order to assess the impact of oxygen concentration upon chemosensitivity (Figure 5). The complexes were compared to the hypoxia-activated pro-drug tirapazamine and to cisplatin.²⁸ Results show that reducing the O₂ concentration gave a general decrease in cytotoxicity for the (O,O) complexes **15** and **18**, with the reduction in activity more pronounced at 0.1% O₂. The iridium (N,O) complex **16** is active under hypoxic conditions albeit less so than under normoxia (21% O₂), with an IC₅₀ value of 20 ± 2 μM at 0.1% O₂. Complex **1** shows a small decrease in its activity in response to low oxygen conditions, but remains highly active even at 0.1% O₂ concentration, confirming its potential as a drug candidate for targeting both normoxic and hypoxic cancer cells.

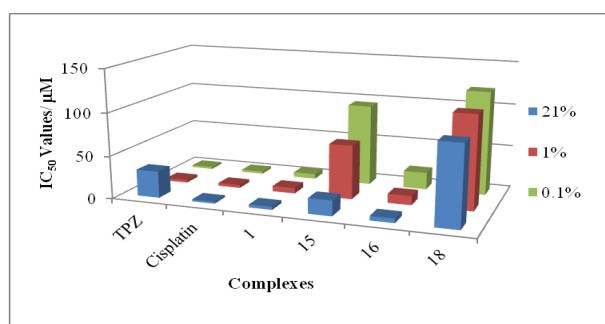


Figure 5 Hypoxic values for complexes **1**, **15**, **16** and **18** against HT-29

The preliminary *in vitro* screening of the complexes indicated that the complexes with a substituents in the *para* position of the β -ketoiminato ligand were highly potent against the cell lines tested (Table 1), and these complexes made good candidates for hypoxia studies. Therefore, in order to further probe the effects of hypoxia on these complexes a range of *para* substituted complexes (**2**, **3**, **8**, **9** and **11**) were tested under hypoxic conditions (Figure 6). Complexes tested at 0.1% O₂ were still active under hypoxic conditions and for all *para* complexes

tested, the anti-cancer activity actually increased at 0.1% O₂, indicating that these complexes are hypoxia sensitive. The most noticeable results were seen for complexes **2** and **8**, which both have nearly 2-fold lower IC₅₀ values under hypoxic conditions. This indicates the potential of these complexes or similar derivatives as hypoxia targeting anti-cancer agents.

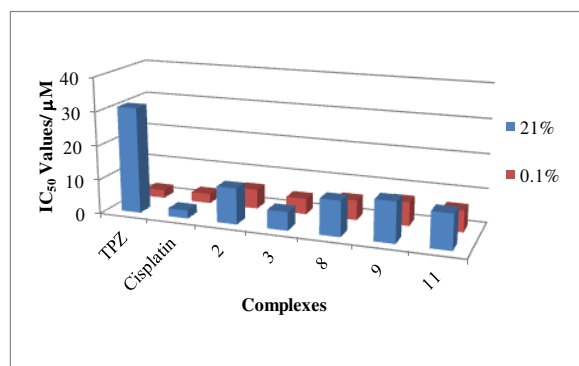


Figure 6 Hypoxic results for complexes **2**, **3**, **8**, **9** and **11** against HT-29

Inhibition of thioredoxin reductase activity

The MTT assay is the gold standard for *in vitro* chemosensitivity studies and IC₅₀ determination but it does not provide any information as to how the drugs may possess their anti-cancer effects. To try and gain some preliminary insight into this, additional assays were conducted for possible effects of the drugs upon, a) thioredoxin reductase activity, b) induction of DNA damage, and, c) induction of cell death. The biological effects of the thioredoxin reductase 1 (Trx-R) system have been shown to contribute to tumour growth and progression.²⁹ Over-expression of thioredoxin reductase 1 has been reported in several tumour types and the enzyme is an important therapeutic target in anti-cancer drug development.³⁰⁻³² In order to investigate the mode of action of our novel complexes, the inhibition of Trx-R activity by complexes **1**, **15**, **16** and **18** was investigated. Previously, a range of iridium picolinamide complexes were found to inhibit Trx-R, with IC₅₀ values in the nanomolar range. However, the analogous ruthenium picolinamide complexes failed to show any enzyme inhibition.³³ In this work, both ruthenium and iridium β -ketoiminato complexes (**1** and **16**) were found to be potent Trx-R inhibitors with IC₅₀ values in the nanomolar range. The β -diketonato complexes **15** and **18** are less active against Trx-R, but still have IC₅₀ values in the low micromolar range (see Figure S3). Trx-R inhibition may thus contribute to the anti-cancer activity of some of our novel complexes; although it is likely that other mechanisms may also be important.

Induction of cancer cell death by apoptosis

The IC₅₀ values determined by chemosensitivity studies using the MTT assay indicate the concentration of drug required for a 50% reduction in viable cell number. Whilst this provides invaluable information on the

activity of the drug against the cell line testing, the MTT assay does not distinguish between effects on cell proliferation and effects on cell survival. Thus, the observed activity of our novel complexes towards the four cancer cell lines could be caused by induction of cell growth arrest or the complexes may actually cause cell death. Cell images under phase contrast microscopy at various time-points after complex addition suggested induction of cell death rather than growth arrest. Using flow cytometry and annexin V/propidium iodide staining the percentage of live cells, early apoptotic cells and late apoptotic/necrotic cells were quantified following incubation of HT-29 or A2780 cells with 10 or 20 μM of complexes **1**, **15**, **16** and **18** for 48 hours (**Figure 7** and **Table S8**).

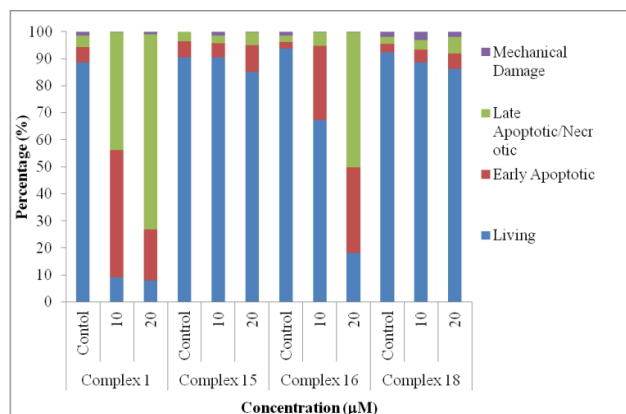
The β -ketoiminato complexes **1** and **16**, which were amongst the most active complexes in the MTT chemosensitivity studies, induced significant levels of apoptotic cell death in both the HT29 (**Figure 7a**) and A2780 (**Figure 7b**) cancer cell lines in a dose-responsive manner. A 48 hour exposure of HT29 cells to 10 μM of the β -ketoinato ruthenium complex **1** resulted in ~50% early apoptotic cells and ~40% late apoptotic/necrotic cells. A 20 μM dose resulted in over 70% of cells staining positive for late apoptosis/necrosis. 20 μM of the active β -ketoiminato iridium complex **16** also induced significant apoptosis, with 31.7% early apoptotic cells and 49.9% late apoptotic or necrotic cells following 48 hour exposure. In contrast, the ruthenium and iridium β -diketonato analogues **15** and **18** respectively, induced only very low levels of apoptosis/necrosis, consistent with their much higher IC_{50} values and lower activity in the chemosensitivity studies (see **Table 1**). Although levels of apoptosis and necrosis were higher than background levels obtained with the controls and higher levels were induced by 20 μM of drug than with 10 μM , even at the highest drug concentration of 20 μM the majority of cells (>84%) were still viable. These observations indicate a clear correlation between IC_{50} value and levels of apoptosis/necrosis induced.

A very similar pattern was also observed for A2780 cells demonstrating that for these two cancer cell lines at least, the ruthenium and iridium β -ketoiminato complexes **1** and **16** induce high levels of cancer cell death by apoptosis, in a dose-dependent manner. This is consistent with their low IC_{50} values and indicates a mechanism by which they are able to exert their *in vitro* anti-cancer activity which merits further future investigation.

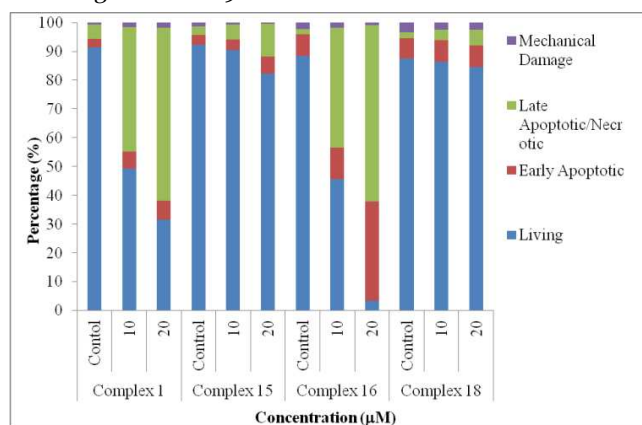
Analysis of cellular DNA damage by the comet assay

Accumulation of cellular DNA damage ultimately leads to the demise of the cell by apoptosis (programmed cell death). As a potential cause of the apoptotic phenotype induced by complexes **1** and **16** (see **Figure 7**) we therefore determined whether the complexes induce any form of cellular DNA damage. Complexes **1**, **15**, **16**, and **18** and cisplatin were tested for induction of double strand

DNA breakage (DSB), single strand DNA breakage (SSB) and DNA cross-linking. Increasing concentrations of the complexes or of cisplatin were incubated with HT-29 cells for 24 hours before harvesting and quantification of the levels of different types of DNA damage in single cells using the either the alkaline or neutral comet assay (see *SI*). None of the complexes induced significant levels of double strand DNA breaks at any of the concentrations tested (**Figure 8a**) and this was also the case for cisplatin, as previously reported.^{34,35}



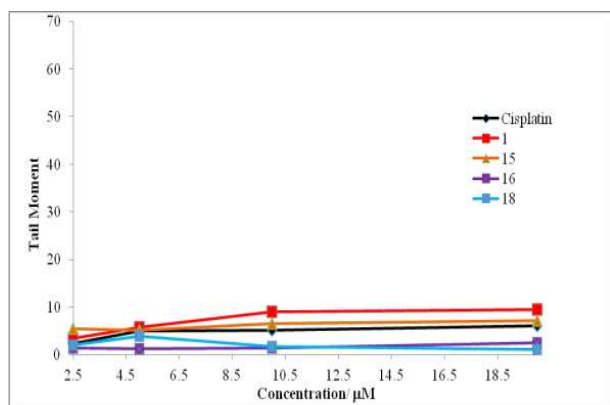
a) Apoptosis results for complexes **1**, **15**, **16** and **18** against HT-29



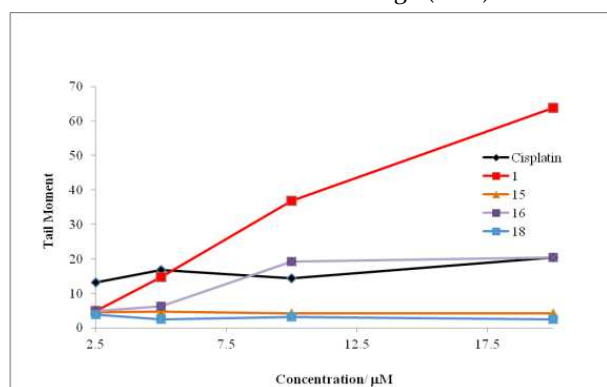
b) Apoptosis results for complexes **1**, **15**, **16** and **18** against A2780

Figure 7 Apoptosis results for complexes **1, **15**, **16** and **18** against HT-29 and A2780**

The complexes also failed to induce DNA cross-linking (see **Figure S4-S6**), whereas cisplatin induced significant DNA cross-linking, consistent with its mechanism of action.³⁶ Importantly however, the ruthenium β -ketoiminato (*N,O*) complex **1** induced high levels of single-strand DNA breaks with levels of SSB damage increasing in a dose-dependent manner with increasing concentrations of complex **1** (**Figure 8b**). In contrast the analogous ruthenium β -diketonato (*O,O*) complex **15** caused no single strand DNA breakage (**Figure 9**) indicating the importance of the binding ligand and consistent with the much lower activity of complex **15** compared to complex **1** in both chemosensitivity studies (**Table 1**) and cell viability analyses (**Figure 7**).



Double Strand Breakage (DSB)



Single strand Breakage (SSB)

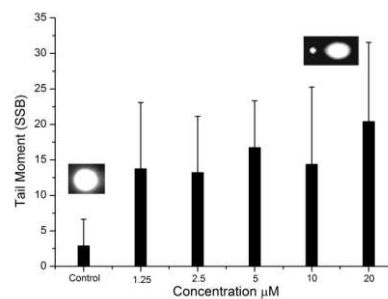
Figure 8 DSB and SSB results for complexes **1**, **15**, **16** and **18** against HT-29

The iridium complexes showed the same general trend, with the β -ketoiminato (N,O) complex **16** also inducing SSB formation similar to its ruthenium analogue (complex **1**) although the extent of DNA damage was less. The iridium β -diketonato (O,O) complex **18**, like its ruthenium β -diketonato counterpart (complex **15**), induced no SSB formation. Thus, for both ruthenium and iridium complexes, the (N,O) ligand appears to be important for complex induction of cellular single strand DNA breaks. Whilst other mechanisms may also be involved, the induction of SSB damage provides a possible cause of the apoptotic phenotype induced by complexes **1** and **16**.

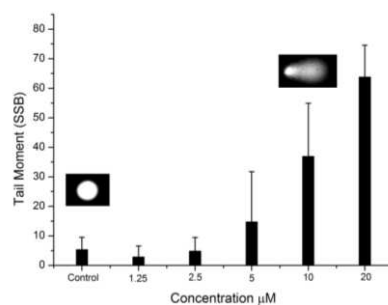
The observation that complexes **1** and **16** induce significant single strand DNA breaks in a dose-dependent manner but few double strand breaks or DNA cross-links (Figures 8, 9 and Figures S4-S6) suggests a different mechanism of action to cisplatin which primarily induces DNA cross-linking. It is also informative with respect to possible combinational chemotherapeutic approaches, suggesting that complexes **1** and **16** may be particularly effective if used in combination with inhibitors of single strand break repair, such as PARP inhibitors. Another approach that may be effective is in combination with

DNA damaging chemotherapeutic agents that work by a different mechanism, for example by inducing DSBs, such as doxorubicin or etoposide. Future studies will investigate how the compounds might induce SSBs, for example by inhibition of topoisomerase I, and will include combinatorial studies with other classes of DNA damaging chemotherapeutic agents for synergistic effects.

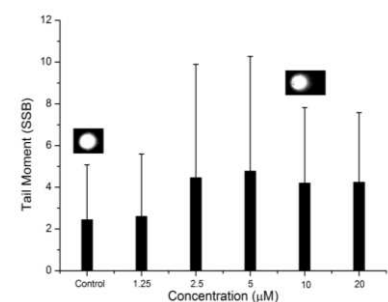
Overall, our results identify the ruthenium and iridium complexes with the β -ketoiminato (N,O) ligand (complexes **1** and **16**) as the most potent and promising of the novel complexes and these are good candidates for future investigation including more detailed mechanistic studies, *in vitro* and *in vivo* ADME studies and analysis of cancer selectivity *in vivo*.



SSB for Cisplatin



SSB for Complex 1



SSB for Complex 15

Figure 9 Bar-charts to tail moment (extent of damage) versus concentration for the SSB assay for a) Cisplatin; b) Complex **1** and c) Complex **15**

Conclusions

From the library of novel ruthenium and iridium complexes tested in this study, our results identify the complexes with a β -ketoiminato ligand as the most active. IC_{50} values varied depending on the complex and cell line

but were typically below 15 μM for all four cancer cell lines tested (HT-29, MCF-7, A2780, A2780cis). Importantly, almost all of the β -ketoiminato complexes were slightly more active than cisplatin against the cisplatin-resistant cell line A2780cis. With complex **1** showing a 3-fold increase in activity when compared to cisplatin. Complexes with the aniline ring removed were tested and results showed this feature to also be essential for potent *in vitro* anti-cancer activity. A selection of complexes were tested under hypoxic (1% O_2) or severely hypoxic (0.1% O_2) conditions against HT-29 cells, and interestingly whereas the β -diketonato complexes tested were significantly less active under hypoxia, many of the β -ketoiminato complexes were more active under hypoxia indicating that these β -ketoiminato complexes are hypoxia-sensitive. As a possible mechanism of action we investigated the inhibition of thioredoxin reductase, with results showing inhibition of this enzyme, with IC_{50} values in the nanomolar range. Further mechanistic investigation showed that the β -ketoiminato complexes fail to induce growth arrest but i) induce significant cancer cell death by apoptosis and, ii) single strand DNA breakage - indicating a different mechanism of action to cisplatin. The selective modifications made to the core 'piano-stool' complex in this study and our initial downstream analyses of the biological effects of this (eg on IC_{50} , cell viability, DNA damage induction) highlight the importance of the size and binding mode of the ligand for activity. The unexpected enhanced activity of many of the β -ketoiminato complexes under hypoxic conditions warrants further investigation but is encouraging in the search for novel anti-cancer agents that are capable of targeting both normoxic and hypoxic cells of a solid tumour.

Experimental

Materials

All chemicals were supplied by Sigma-Aldrich Chemical Co., Acros Organics, Strem Chemical Co. and BOC gases. Functionalised β -diketonate and β -ketoiminato ligands were prepared by adaptations of literature methods.^{19,20} Deuterated NMR solvents were supplied by Sigma-Aldrich Chemical Co. or Acros Organics.

Analysis

All NMR spectra were recorded by either the author or Mr Simon Barrett on a Bruker DPX 300 or a Bruker DPX 500 spectrometer. Microanalyses were recorded by Mr. Ian Blakeley or Ms Tanya Marinko-Covell at the University of Leeds Microanalytical Service. Mass Spectra were recorded by either Ms. Tanya Marinko-Covell or the author, on a Micromass ZMD spectrometer with electrospray ionisation and photoiodide array analyser at the University of Leeds Mass Spectrometry Service.

Elemental Analysis

All biologically evaluated compounds must demonstrate a purity >95%, and therefore the compounds synthesised within this report have been analysed using elemental (CHN)

analysis, by means of combustion. This technique requires the sample to be burned in an excess of oxygen and has a variety of traps which collect the combustion products: CO_2 , H_2O and NO . These masses are then used to help calculate the masses of the 'unknown' product. The experimental values are compared with the calculated values of the sample, and all synthesised compounds herein are within 0.5% of the calculated values.

X-ray Crystallography

A suitable single crystal was selected and immersed in an inert oil. The crystal was then mounted on a glass capillary or nylon loop and attached to a goniometer head on a Bruker X8 Apex diffractometer using graphite monochromated $\text{Mo-K}\alpha$ radiation ($\lambda = 0.71073 \text{ \AA}$) or an Agilent SuperNova diffractometer using mirror monochromated $\text{Mo-K}\alpha$ radiation ($\lambda = 0.71073 \text{ \AA}$), using 1.0° ϕ -rotation frames. The crystal was cooled to between 100-173 K by an Oxford Cryostream low temperature device.³⁷ The full data sets were recorded and the images processed using DENZO and SCALEPACK programs³⁸ or Crysalis Pro software.³⁹

Structure solution by direct methods was achieved through the use of SHELXS programs,⁴⁰ and the structural model refined by full matrix least squares on F^2 using SHELXL97. Unless otherwise stated, hydrogen atoms were placed using idealised geometric positions (with free rotation for methyl groups), allowed to move in a "riding model" along with the atoms to which they were attached, and refined isotropically. Molecular graphics were plotted using POV-Ray⁴¹ via the XSeed program⁴⁰ and OLEX2.⁴² Editing of CIFs and construction of tables of bond lengths and angles were achieved using WC⁴³ and PLATON.⁴⁴

Synthesis

Ligands L2-L12

All ligands were synthesised by dissolving the corresponding functionalised β -diketonate (0.5 g) in toluene (10 mL), followed by addition of aniline (1 mL) and HCl (0.5 mL). The mixture was stirred overnight and the precipitate filtered under reduced pressure. The solvent was removed from the filtrate and then recrystallised from hot ethanol to yield analytically pure compounds.

Ligand L2 (0.63 g, 2.5 mmol, 87%)

^1H NMR (CDCl_3 , 300 MHz, 300 K) δ 13.05 (s, 1H, NH), 7.94 (v. dd, 2H, CH, $^3J(\text{H-H}) = 9.2 \text{ Hz}$ and $^3J(\text{H-}^{19}\text{F}) = 2.3 \text{ Hz}$), 7.39 (br. t, 2H, CH, $^3J(\text{H-H}) = 7.9 \text{ Hz}$), 7.24 (br. t, 1H, CH, $^3J(\text{H-H}) = 7.6 \text{ Hz}$), 7.19 (br. d, 2H, CH, $^3J(\text{H-H}) = 7.2 \text{ Hz}$), 7.11 (v. t, 2H, CH, $^3J(\text{H-H}) = 8.7 \text{ Hz}$ and $^4J(\text{H-}^{19}\text{F}) = 1.9 \text{ Hz}$), 5.85 (s, 1H, methine CH, H₉), 2.15 (s, 1H, aliphatic CH₃). $^{13}\text{C}\{^1\text{H}\}$ NMR (CDCl_3 , 75 MHz, 300K) δ 187.2 (Q), 164.5 (d, Q C-F, $^1J(^{13}\text{C-}^{19}\text{F}) = 249.7 \text{ Hz}$), 162.4 (Q), 138.5 (Q), 129.3 (d, 2 x CH, $^3J(^{13}\text{C-}^{19}\text{F}) = 8.7 \text{ Hz}$), 129.2 (2 x CH), 125.9 (CH), 124.8 (2 x CH), 115.2 (d, 2 x CH, $^3J(^{13}\text{C-}^{19}\text{F}) = 21.0 \text{ Hz}$), 93.8 (methine CH), 20.4 (aliphatic CH₃). Analysis Calculated for $\text{C}_{16}\text{H}_{14}\text{FNO}$: C 74.30 H 5.53, N 5.49% Analysis Found for $\text{C}_{16}\text{H}_{14}\text{FNO}$: C 74.35, H 5.40, N 5.25% ES MS (+): m/z 255.6 [M^+]

Ligand L3 (0.35 g, 1.0 mmol, 51%)

^1H NMR (CDCl_3 , 300 MHz, 300 K) δ 13.12 (s, 1H, NH), 7.90 (d, 2H, CH, $^3J(\text{H-H}) = 8.5 \text{ Hz}$), 7.44 (d, 2H, CH, $^3J(\text{H-H}) = 8.5$

Hz), 7.42 (m, 1H, CH), 7.25 (d, 2H, CH, $^3J(\text{H-H}) = 7.5$ Hz), 7.22 (m, 2H, CH, $^3J(\text{H-H}) = 8.5$ Hz), 5.89 (s, 1H, methine CH), 2.19 (s, 3H, aliphatic CH₃) ¹³C{¹H} NMR (CDCl₃, 75MHz, 300K) δ 163.1 (Q), 137.4 (Q), 129.6 (CH), 128.9 (CH), 126.4 (CH), 125.3 (CH), 98.4 (methine CH), 20.8 (aliphatic CH₃) Analysis Calculated for C₁₆H₁₄ClNO: C 70.70, H 5.19, N 5.20, Cl 13.10% Analysis Found for C₁₆H₁₄ClNO: C 70.70, H 5.25, N 5.40, Cl 12.80% ES MS (+): *m/z* 272.0 [MH⁺]

Ligand L4 (0.58 g, 2.0 mmol, 88%)

¹H NMR (CDCl₃, 300 MHz, 300 K) δ 12.86 (s, 1H, NH), 7.51 (d, 1H, CH, $^3J(\text{H-H}) = 8.4$ Hz), 7.46 (d, 2H, CH), 7.42 (d, 1H, CH, $^3J(\text{H-H}) = 7.8$ Hz), 7.33-7.30 (m, 3H, CH), 7.24 (d, 2H, CH, $^3J(\text{H-H}) = 8.7$ Hz), 5.89 (s, 1H, methine CH), 2.14 (s, 3H, aliphatic CH₃) ¹³C{¹H} NMR (CDCl₃, 75MHz, 300K) δ 188.7 (Q), 163.3 (Q), 139.9 (Q), 138.6 (Q), 135.7 (Q), 132.2 (Q), 130.7 (CH), 130.4 (CH), 129.7 (2 x CH), 127.4 (CH), 126.7 (CH), 125.4 (2 x CH), 98.5 (methine CH), 20.6 (aliphatic CH₃) Analysis Calculated for C₁₆H₁₃Cl₂NO: C 62.809, H 4.28, N 4.60, Cl 23.20% Analysis Found for C₁₆H₁₃Cl₂NO: C 62.70, H 4.25, N 4.50, Cl 22.0% ES MS (+): *m/z* 306.1 [MH⁺]

Ligand L5 (0.46 g, 2.2 mmol, 68%)

H NMR (CDCl₃, 300 MHz, 300 K) δ 12.71 (s, 1H, NH), 7.43 (m, 1H, CH), 7.33 (br. t, 2H, CH, $^3J(\text{H-H}) = 7.5$ Hz), 7.24 (br. s, 1H, CH), 7.21-7.16 (m, 2H, CH), 7.13(d, 2H, CH, $^3J(\text{H-H}) = 7.5$ Hz), 5.43 (s, 1H, methine CH), 2.03 (s, 3H, aliphatic CH₃) ¹³C{¹H} NMR (CDCl₃, 75 MHz, 300 K) δ 187.8 (Q), 163.2 (Q), 142.4 (Q), 138.1 (Q), 132.6 (Q C-Cl), 131.3 (CH), 130.0 (CH), 129.3 (CH), 126.4 (CH), 125.1 (CH), 97.9 (methine CH), 20.2 (aliphatic CH₃) Analysis Calculated for C₁₆H₁₃Cl₂NO: C 62.67, H 4.29, N 4.58, Cl 23.15% Analysis Found for C₁₆H₁₃Cl₂NO: C 62.65, H 4.20, N 4.45, Cl 23.30 ES MS (+): *m/z* 306.2 [M⁺]

Ligand L6 (0.10 g, 0.29 mmol, 55%)

¹H NMR (CDCl₃, 500.23 MHz, 300.1 K) δ 12.75 (br. s, 1H, NH), 7.43-7.39 (m, 3H, 3 x CH), 7.33 (d, 1H, CH, $^3J(\text{H-H}) = 8.2$ Hz), 7.29 (br. d, 1H, CH, $^3J(\text{H-H}) = 7.3$ Hz), 7.22 (br. d, 2H, CH, $^3J(\text{H-H}) = 7.6$ Hz), 5.45 (s, 1H, methine CH), 2.11 (s, 3H, aliphatic CH₃) ¹³C{¹H} NMR (CDCl₃, 125.9 MHz, 300.0 K) δ 187.9 (Q), 163.4 (Q), 141.6 (Q), 138.0 (Q), 134.5 (Q C-Cl), 132.4 (Q C-Cl), 131.0 (Q C-Cl), 129.3 (CH), 128.4 (CH), 126.9 (CH), 126.4 (CH), 125.1 (CH), 97.8 (methane CH), 20.2 (CH₃) Analysis Calculated for C₁₆H₁₂Cl₃NO: C 56.42, H 3.55, Cl 31.22, N 4.11% Analysis Found for C₁₆H₁₂Cl₃NO: C 56.25, H 3.45, Cl 31.05, N 4.05% ES MS (+): *m/z* 340.0 [M⁺]

Ligand L7 (0.42 g, 1.3 mmol, 62%)

¹H NMR (CDCl₃, 300 MHz, 300 K) δ 13.08 (s, 1H, NH), 8.06 (t, 1H, CH, $^4J(\text{H-H}) = 1.7$ Hz), 7.84 (br. dt, 1H, CH, $^3J(\text{H-H}) = 8.0$ Hz and $^3J(\text{H-H}) = 1.5$ Hz), 7.59 (dq, 1H, CH, $^3J(\text{H-H}) = 7.9$ Hz and $^4J(\text{H-H}) = 0.9$ (x3) Hz), 7.40 (br. t, 2H, CH, $^3J(\text{H-H}) = 8.1$ Hz) 7.31 (t, 1H, CH, $^3J(\text{H-H}) = 7.9$ Hz), 7.25 (br. t, 1H, CH, $^3J(\text{H-H}) = 7.2$ Hz), 7.20 (br. d, 2H, CH, $^3J(\text{H-H}) = 7.5$ Hz), 5.83 (s, 1H, methine CH), 2.16 (s, 3H, aliphatic CH₃) ¹³C{¹H} NMR (CDCl₃, 75 MHz, 300 K) δ 186.7(Q), 163.0 (Q), 142.0 (2 x Q), 138.4 (Q C-Br), 133.6 (CH), 130.2 (CH), 129.8 (CH), 129.2 (CH), 126.1 (CH), 125.6 (CH), 124.9 (CH), 94.0 (methine CH), 20.4 (aliphatic CH₃) Analysis Calculated for C₁₆H₁₄BrNO: C 60.76, H 4.47, N 4.43% Analysis Found for C₁₆H₁₄BrNO: C 60.80, H 4.45, N 4.43% ES MS (+): *m/z* 316.3 [M⁺]

Ligand L8 (0.44 g, 1.0 mmol, 67%)

¹H NMR (CDCl₃, 300 MHz, 300 K) δ 12.42 (s, 1H, NH), 7.73 (d, 2H, CH, $^3J(\text{H-H}) = 7.2$ Hz), 7.56 (m, 1H, CH), 7.45 (d, 2H, CH), 7.42 (d, 1H, CH, $^3J(\text{H-H}) = 7.5$ Hz) 7.37 (d, 2H, CH, $^3J(\text{H-H}) = 8.0$ Hz), 5.87 (s, 1H, methine CH), 2.19 (s, 3H, aliphatic CH₃) ¹³C{¹H} NMR (CDCl₃, 75 MHz, 300 K) δ 173.9 (Q), 134.9 (Q), 131.9 (2 x CH), 130.4 (2 x CH), 129.9 (2 x CH), 126.8 (CH), 125.0 (2 x CH), 102.2 (methane CH), 22.1 (aliphatic CH₃) Analysis Calculated for C₁₆H₁₄BrNO: C 60.80, H 4.46, N 4.40% Analysis Found for C₁₆H₁₄BrNO: C 61.10, H 5.05, N 4.40% ES MS (+): *m/z* 316.0 [MH⁺]

Ligand L9 (0.76 g, 2.1 mmol, 76%)

¹H NMR (CDCl₃, 500.23 MHz, 300.1 K) δ 13.09 (br. s, 1H, NH), 7.79 (d, 2H, CH, $^3J(\text{H-H}) = 8.3$ Hz), 7.65 (d, 2H, CH, $^3J(\text{H-H}) = 8.3$ Hz), 7.39 (br. t, 2H, CH, $^3J(\text{H-H}) = 7.8$ Hz), 7.25 (br. t, 1H, CH, $^3J(\text{H-H}) = 7.3$ Hz), 7.19 (br. d, 2H, CH, $^3J(\text{H-H}) = 7.3$ Hz), 5.84 (s, 1H, methine CH), 2.15 (s, 3H, aliphatic CH₃) ¹³C{¹H} NMR (CDCl₃, 75 MHz, 300 K) δ 187.4 (Q), 162.8 (Q), 139.4 (2 x Q), 138.4 (Q C-I), 137.5 (2 x CH), 129.2 (2 x CH), 128.7 (2 x CH), 126.0 (CH), 124.9 (2 x CH), 93.8 (methine CH), 20.4 (aliphatic CH₃) Analysis Calculated for C₁₆H₁₄INO: C 52.91, H 3.89, I 34.94, N 3.86% Analysis Found for C₁₆H₁₄INO: C 52.95, H 4.10, I 34.65, N 3.75% ES MS (+): *m/z* 364.0 [MH⁺]

Ligand L10 (0.40 g, 1.4 mmol, 38%)

¹H NMR (CDCl₃, 500.13 MHz, 319.2 K) δ 13.01 (br. s, 1H, NH), 7.91 (br. d, 2H, CH, $^3J(\text{H-H}) = 8.8$ Hz), 7.39-7.34 (br. t, 2H, CH, $^3J(\text{H-H}) = 7.3$ Hz), 7.23-7.20 (m, 1H, CH), 7.18 (br. d, 2H, CH, $^3J(\text{H-H}) = 8.8$ Hz), 5.86 (s, 1H, methine CH), 4.11 (q, 2H, ethoxy CH₂, $^3J(\text{H-H}) = 6.7$ Hz), 2.14 (s, 3H, aliphatic CH₃), 1.45 (t, 3H, ethoxy CH₃, $^3J(\text{H-H}) = 6.7$ Hz) ¹³C{¹H} NMR (CDCl₃, 75.5 MHz, 300.0 K) δ 187.9 (Q), 161.4 (Q), 138.9 (2 x Q), 132.5 (Q), 129.1 (2 x CH), 129.0 (2 x CH), 125.5 (CH), 124.7 (2 x CH), 114.0 (2 x CH), 93.8 (methine CH), 63.6 (ethoxy CH₂), 20.5 (aliphatic CH₃), 14.8 (ethoxy CH₃) Analysis Calculated for C₁₈H₁₉NO: C 75.23, H 5.65, N 13.85 Analysis Found for C₁₈H₁₉NO: C 74.75, H 5.70, N 13.80 ES MS (+): *m/z* 282.15 [MH⁺]

Ligand L11 (0.42 g, 1.7 mmol, 59%)

¹H NMR (CDCl₃, 500.13 MHz, 319.2 K) δ 13.12 (br. s, 1H, NH), 7.87 (d, 2H, CH, $^3J(\text{H-H}) = 8.2$ Hz), 7.41 (d, 2H, CH, $^3J(\text{H-H}) = 7.6$ Hz), 7.28 (m, 2H, CH), 7.25 (m, 2H, CH), 7.23 (m, 1H, CH), 5.89 (s, 1H, methine CH), 2.44 (s, 3H, aliphatic CH₃), 2.19 (s, 3H, methyl CH₃) ¹³C{¹H} NMR (CDCl₃, 75.5 MHz, 300.0 K) δ 189.0 (Q), 162.2 (Q), 141.7 (Q), 139.2 (Q), 137.7 (Q), 129.7 (2 x CH), 129.4 (2 x CH), 127.5 (CH), 126.1 (CH), 125.1 (2 x CH), 94.5 (methine CH), 21.9 (aliphatic CH₃), 20.9 (methyl CH₃) Analysis Calculated for C₁₇H₁₇NO: C 81.20, H 6.82, N 5.60% Analysis Found for C₁₇H₁₇NO: C 79.80, H 6.80, N 5.10 ES MS (+): *m/z* 252.20 [MH⁺]

Ligand 12 (0.65 g, 2.3 mmol, 81%)

¹H NMR (CDCl₃, 500 MHz, 300.0 K) δ 13.13 (br. s, 1H, NH), 8.51 (d, 2H, CH, $^3J(\text{H-H}) = 8.3$ Hz), 7.89 (br. t, 2H, CH, $^3J(\text{H-H}) = 8.3$ Hz), 7.70 (br. d, 1H, CH, $^4J(\text{H-H}) = 6.9$ Hz), 7.57-7.53 (m, 1H, CH), 7.53-7.48 (m, 2H, CH), 7.42 (br. t, 2H, CH, $^3J(\text{H-H}) = 8.3$ Hz), 7.28-7.25 (m, 2H, CH), 5.70 (s, 1H, methine CH), 2.16 (s, 3H, aliphatic CH₃) ¹³C{¹H} NMR (CDCl₃, 125 MHz, 300 K) δ 193.0 (Q), 162.0 (Q), 143.2 (Q), 140.1 (Q), 138.6 (2 x Q), 130.3 (CH), 129.9 (CH), 129.2 (CH), 128.4 (CH), 126.6 (CH), 126.1 (CH), 125.4 (CH), 124.9 (CH), 124.9 (CH),

99.0 (methine CH), 20.3 (aliphatic CH₃) Analysis Calculated for C₂₀H₁₇NO: C 83.59, H 5.96, N 4.87% Analysis Found for C₂₀H₁₇NO: C 83.70, H 6.00, N 4.80% ES MS (+): m/z 288.14 [MH⁺]

Ligand L13 (0.56 g, 1.9 mmol, 64%)

¹H NMR (CDCl₃, 300.13 MHz, 300.0 K) δ 12.90 (br. s, 1H, NH), 7.97-7.92 (m, 2H, CH), 7.16-7.09 (m, 3H, 3 x CH), 6.99 (ddd, 1H, CH, 3J (H-H) = 9.0 Hz and 3J (H-F) = 3.1 and 2.0 Hz), 6.93-6.87 (m, 1H, CH), 5.95 (s, 1H, methine CH), 2.17 (s, 3H, aliphatic CH₃) ¹³C{¹H} NMR (CDCl₃, 125.9 MHz, 300.0 K) δ 188.1 (Q), 164.8 (d, Q, C-F, 1J (C-F) = 250.5 Hz), 161.5 (Q), 158.3 (dd, Q C-F, 1J (C-F) = 242.3 Hz and 4J (C-F) = 3.1 Hz), 152.7 (dd, Q C-F, 1J (C-F) = 242.3 Hz and 4J (C-F) = 3.1 Hz), 135.7 (d, Q, 4J (C-F) = 3.1 Hz), 129.6 (d, 2 x CH, 3J (C-F) = 8.3 Hz), 127.9 (dd, Q, 2J (C-F) = 24.7 Hz and 3J (C-F) = 4.1 Hz), 115.3 (d, 3 x CH, 3J (C-F) = 21.7 Hz), 113.1 (d, CH, 3J (C-F) = 23.7 Hz), 113.0 (d, CH, 2J (C-F) = 25.8 Hz), 95.3 (methine CH), 20.3 (aliphatic CH₃) Analysis Calculated for C₁₆H₁₂F₃NO: C 65.98, H 4.15, N 4.81% Analysis Found for C₁₆H₁₂F₃NO: C 65.35, H 4.35, N 4.70% ES MS (+): m/z 292.09 [MH⁺]

Ligand L14

This ligand was prepared as previously reported by Roshchupkina *et al.*¹⁸

Complexes 2-13

Complexes 2-13 were synthesised by addition of [p-cymRuCl₂]₂ (1 eq), a functionalised β-ketoiminate ligand (2 eq) and Et₃N (2 eq). All were stirred in dichloromethane (30 mL) at room temperature overnight. The solvent was removed under reduced pressure and the crude product recrystallised using slow evaporation from a methanolic solution.

Complex 2 (0.07 g, 0.13 mmol, 54%)

¹H NMR (CDCl₃, 500.57 MHz, 300.0 K) δ 7.84 (d, 2H, CH, 3J (H-H) = 9.0 Hz and 4J (H-H) = 2.2 Hz), 7.75 (br. d, 1H, CH, 3J (H-H) = 9.0 Hz), 7.43 (br. t, 2H, CH, 3J (H-H) = 7.7 Hz), 7.26-7.22 (br. dd, 1H, CH, 3J (H-H) = 6.2 Hz and 4J (H-H) = 2.1 Hz), 7.09 (br. d, 1H, CH, 3J (H-H) = 6.9 Hz), 7.03-6.99 (a. t (v. dd), 2H, CH, 3J (H-H) = 8.6 Hz and 4J (H-H) = 3.9 Hz), 5.37 (s, 1H, methine CH), 5.35 (br. d, 1H, CH, 3J (H-H) = 6.0 Hz), 5.16 (br. d, 1H, CH, 3J (H-H) = 6.0 Hz), 5.06 (br. d, 1H, CH, 3J (H-H) = 5.6 Hz), 2.67 (br. sept, 1H, CH(CH₃)₂, 3J (H-H) = 6.9 Hz), 2.03 (s, 3H, methyl CH₃), 1.79 (s, 3H, aliphatic CH₃), 1.20 (a. t (v. dd), 6H, CH(CH₃)₂, 3J (H-H) = 7.5 Hz) ¹³C{¹H} NMR (CDCl₃, 125.9 MHz, 300.0 K) δ (170.6 (Q), 164.8 (Q), 163.6 (d, Q C-F, 1J (C-F) = 247.4 Hz), 157.2 (Q), 137.5 (Q), 129.6 (2 x CH), 128.2 (d, 2 x CH, 3J (C-F) = 7.3 Hz), 126.1 (CH), 125.4 (CH), 123.9 (CH), 114.6 (d, 2 x CH, 2J (C-F) = 21.7 Hz), 100.8 (Q), 96.2 (Q), 94.2 (methine CH), 87.0 (CH), 84.6 (CH), 84.5 (CH), 79.4 (CH), 30.5 (CH(CH₃)₂), 24.7 (aliphatic CH₃), 23.6 (CH(CH₃)₂), 20.9 (CH(CH₃)₂), 18.3 (methyl CH₃) Analysis Calculated for C₂₆H₂₇ClF₃NORu: C 59.48, H 5.18, N 2.67% Analysis Found for C₂₆H₂₇ClF₃NORu: C 59.25, H 5.20, N 2.75% ES MS (+): m/z 490.11 [M⁺]-Cl

Complex 3 (0.06 g, 0.11 mmol, 62%)

¹H NMR (CDCl₃, 500.23 MHz, 299.9 K) δ 7.81-7.77 (br. dt, CH, 3J (H-H) = 8.7 Hz and 4J (H-H) = 1.8 Hz), 7.74 (br. d,

1H, CH, 3J (H-H) = 7.5 Hz), 7.43 (br. t, 2H, CH, 3J (H-H) = 8.3 Hz), 7.30 (br. dt, 2H, CH, 3J (H-H) = 8.7 Hz and 4J (H-H) = 2.0 Hz), 7.26-7.22 (br. t, 1H, CH, 3J (H-H) = 7.5 Hz), 7.09 (br. d, 1H, CH, 3J (H-H) = 6.8 Hz), 5.39 (s, 1H, methine CH), 5.35 (br. d, CH, 3J (H-H) = 6.0 Hz), 5.16 (br. d, 1H, CH, 3J (H-H) = 6.0 Hz), 5.06 (br. d, 1H, CH, 3J (H-H) = 5.6 Hz), 3.68 (br. d, 1H, CH, 3J (H-H) = 5.6 Hz), 2.67 (br. sept, 1H, CH(CH₃)₂, 3J (H-H) = 7.0 Hz), 2.03 (s, 3H, methyl CH₃), 1.79 (s, 3H, aliphatic CH₃), 1.21 (d, 3H, CH(CH₃)₂, 3J (H-H) = 9.9 Hz), 1.91 (d, 3H, CH(CH₃)₂, 3J (H-H) = 9.9 Hz) ¹³C{¹H} NMR (CDCl₃, 75.5 MHz, 300.1 K) δ 170.3 (Q), 164.9 (Q), 157.2 (Q), 138.0 (Q), 135.2 (Q), 129.6 (CH), 128.2 (CH), 128.0 (CH), 127.8 (CH), 126.0 (CH), 125.5 (CH), 123.3 (CH), 104.4 (Q), 96.3 (Q), 94.5 (methine CH), 87.1 (CH), 84.6 (CH), 84.7 (CH), 84.7 (CH), 79.5 (CH), 30.5 (CH(CH₃)₂), 24.7 (aliphatic CH₃), 23.6 (CH(CH₃)₂), 20.9 (CH(CH₃)₂), 18.4 (methyl CH₃) Analysis Calculated for C₂₆H₂₇Cl₂NORu: C 57.67, H 5.03, N 2.59, Cl 13.09% Analysis Found for C₂₆H₂₇Cl₂NORu: C 57.40, H 5.00, N 2.40, Cl 13.05% ES MS (+): m/z 506.08 [M⁺]-Cl

Complex 4 (0.06 g, 0.11 mmol, 62%)

¹H NMR (CDCl₃, 500.13 MHz, 240.2 K) δ 7.72 (br. d, 1H, CH, 3J (H-H) = 7.8 Hz), 7.45 (br. d, 2H, CH, 3J (H-H) = 6.2 Hz), 7.35 (br. d, 1H, CH, 3J (H-H) = 5.9 Hz), 7.32 (br. d, 1H, CH, 3J (H-H) = 8.2 Hz), 7.26-7.23 (m, 1H, CH), 7.20 (br. dd, 1H, CH, 3J (H-H) = 8.2 Hz and 4J (H-H) = 1.9 Hz), 5.30 (br. d, 1H, CH), 5.22 (br. d, 1H, CH, 3J (H-H) = 6.0 Hz), 5.01 (br. d, 1H, CH, 3J (H-H) = 5.2 Hz), 4.93 (s, 1H, methine CH), 3.44 (br. d, 1H, CH, 3J (H-H) = 5.1 Hz), 2.74 (br. sept, CH(CH₃)₂, 3J (H-H) = 6.6 Hz), 2.05 (s, 3H, methyl CH₃), 1.74 (s, 3H, aliphatic CH₃), 1.27 (br. d, 3H, CH(CH₃)₂, 3J (H-H) = 6.7 Hz), 1.22 (br. d, 3H, CH(CH₃)₂, 3J (H-H) = 6.7 Hz) ¹³C{¹H} NMR (CDCl₃, 125.8 MHz, 240.2 K) δ 171.5 (Q), 164.3 (Q), 156.7 (Q), 138.5 (Q), 133.9 (Q C-Cl), 131.4 (Q C-Cl), 130.9 (CH), 129.6 (CH), 129.1 (CH), 127.8 (CH), 126.7 (CH), 125.2 (CH), 99.6 (Q), 98.1 (methine CH), 97.2 (Q), 87.8 (CH), 83.4 (CH), 83.2 (CH), 79.9 (CH), 30.1 (CH(CH₃)₂), 24.6 (aliphatic CH₃), 23.8 (CH(CH₃)₂), 21.1 (CH(CH₃)₂), 18.8 (methyl CH₃) Analysis Calculated for C₂₆H₂₆Cl₃NORu: C 54.22, H 4.55, N 2.43, Cl 18.47% Analysis Found for C₂₆H₂₆Cl₃NORu: C 54.05, H 4.65, N 2.35, Cl 18.45% ES MS (+): m/z 540.04 [M⁺]-Cl

Complex 5 (0.32 g, 0.56 mmol 61%)

¹H NMR (CDCl₃, 300.13 MHz, 295.5 K) δ (7.78-7.73 (m, 1H, CH), 7.47-7.43 (br. d, 2H, CH), 7.42 (m, 1H, CH), 7.25 (d, 2H, CH, 3J (H-H) = 7.0 Hz), 7.21-7.16 (m, 1H, CH), 7.13-7.08 (m, 1H, CH), 5.28 (br. d, 1H, CH, 3J (H-H) = 6.2 Hz), 5.14 (br. d, 1H, CH, 3J (H-H) = 6.2 Hz), 5.02 (br. d, 1H, CH, 3J (H-H) = 5.5 Hz), 4.94 (s, 1H, methine CH), 3.64 (br. d, 1H, CH, 3J (H-H) = 5.7 Hz), 2.76 (br. sept, 1H, CH(CH₃)₂, 3J (H-H) = 7.0 Hz), 2.07 (s, 3H, methyl CH₃), 1.74 (s, 3H, aliphatic CH₃), 1.28 (br. d, 3H, CH(CH₃)₂, 3J (H-H) = 6.8 Hz), 1.22 (br. d, 3H, CH(CH₃)₂, 3J (H-H) = 7.0 Hz) ¹³C{¹H} NMR (CDCl₃, 75.5 MHz, 295.6 K) δ 171.4 (Q), 164.9 (Q), 156.9 (Q, 2 x C-Cl), 141.7 (Q), 132.3 (Q), 130.6 (CH), 130.2 (CH), 129.0 (CH), 127.0 (CH), 125.8 (CH), 125.6 (CH), 123.2 (CH), 100.7 (Q), 98.5 (methine CH), 97.2 (Q), 87.0 (CH), 83.7 (CH), 83.5 (CH), 80.4 (CH), 30.3 (CH(CH₃)₂), 24.3 (aliphatic CH₃), 23.5 (CH(CH₃)₂), 21.4 (CH(CH₃)₂), 18.6 (methyl CH₃) Analysis Calculated for C₂₆H₂₆Cl₃NORu: C 54.22, H 4.55, N 2.43, Cl 18.47% Analysis Found for C₂₆H₂₆Cl₃NORu: C 53.95, H 4.50, N 2.35, Cl 18.70% ES MS (+): m/z 540.05 [M⁺]-Cl

Complex 6 (0.06g, 0.10 mmol, 60%)

^1H NMR (CDCl_3 , 300.13 MHz, 300.0 K) δ 7.75 (dd, 1H, CH , 3J (^1H - ^1H)= 7.3 Hz, 4J (^1H - ^1H)= 1.6 Hz), 7.45 (br. t, 2H, CH , 3J (^1H - ^1H)= 8.5 Hz), 7.34 (d, 1H, CH , 3J (^1H - ^1H)= 8.3 Hz), 7.27-7.22 (m, 2H, CH), 7.14-7.09 (m, 1H, CH), 5.27 (br. d, 1H, CH , 3J (^1H - ^1H)= 6.2 Hz), 5.12 (br. d, 1H, CH , 3J (^1H - ^1H)= 6.2 Hz), 5.03 (br. d, 1H, CH , 3J (^1H - ^1H)= 5.7 Hz), 4.88 (s, 1H, methine CH), 3.63 (br. d, 1H, CH , 3J (^1H - ^1H)= 5.7 Hz), 2.76 (br. sept, 1H, $\text{CH}(\text{CH}_3)_2$, 3J (^1H - ^1H)= 7.0 Hz), 2.07 (s, 3H, methyl CH_3), 1.74 (s, 3H, aliphatic CH_3), 1.30 (d, 3H, $\text{CH}(\text{CH}_3)_2$, 3J (^1H - ^1H)= 6.8 Hz), 1.23 (d, 3H, $\text{CH}(\text{CH}_3)_2$, 3J (^1H - ^1H)= 7.0 Hz) $^{13}\text{C}\{^1\text{H}\}$ NMR (CDCl_3 , 75.5 MHz, 295.6 K) δ 171.7 (Q), 165.0 (Q), 156.9 (Q), 141.0 (Q), 133.4 (Q, C-Cl), 131.5 (Q, C-Cl), 130.9 (Q, C-Cl, C_{22-24}), 129.7 (2 x CH), 128.5 (CH), 128.1 (CH), 127.8 (CH), 125.6 (CH), 123.2 (CH), 100.8 (Q), 98.5 (methine CH), 97.2 (Q), 87.0 (CH), 83.8 (CH), 83.7 (CH), 80.4 (CH), 30.3 ($\text{CH}(\text{CH}_3)_2$), 24.3 (aliphatic CH_3), 23.6 ($\text{CH}(\text{CH}_3)_2$), 21.4 ($\text{CH}(\text{CH}_3)_2$), 18.6 (methyl CH_3) Analysis Calculated for $\text{C}_{26}\text{H}_{25}\text{Cl}_4\text{NORu}$: C 51.16, H 4.13, N 2.29, Cl 23.23 % Analysis Found for $\text{C}_{26}\text{H}_{25}\text{Cl}_4\text{NORu}$: C 51.00, H 4.15, N 2.20, Cl 23.20% ES MS (+): m/z 574.00 [M^+]-Cl

Complex 7 (0.31 g, 0.54 mmol, 71%)

^1H NMR (CDCl_3 , 500.23 MHz, 300.0 K) δ 8.00 (br. t, 1H, CH , 4J (^1H - ^1H)= 1.6 Hz), 7.76-7.73 (br. d, 2H, CH , 3J (^1H - ^1H)= 8.0 Hz), 7.48 (br. d, 1H, CH , 3J (^1H - ^1H)= 7.6 Hz), 7.43 (br. t, 2H, CH , 3J (^1H - ^1H)= 7.5 Hz), 7.24 (br. t, 1H, CH , 3J (^1H - ^1H)= 7.6 Hz), 7.20 (t, 1H, CH , 3J (^1H - ^1H)= 7.9 Hz), 7.09 (d, 1H, CH , 3J (^1H - ^1H)= 6.4 Hz), 5.38 (s, 1H, methine CH), 5.35 (br. d, 1H, CH , 3J (^1H - ^1H)= 6.4 Hz), 5.17 (br. d, 1H, CH , 3J (^1H - ^1H)= 6.0 Hz), 5.07 (br. d, 1H, CH , 3J (^1H - ^1H)= 5.6 Hz), 3.69 (br. d, 1H, CH , 3J (^1H - ^1H)= 5.6 Hz), 2.67 (br. sept, 1H, $\text{CH}(\text{CH}_3)_2$), 2.03 (s, 3H, methyl CH_3), 1.79 (s, 3H, aliphatic CH_3), 1.22 (d, 3H, $\text{CH}(\text{CH}_3)_2$, 3J (^1H - ^1H)= 7.1 Hz), 1.20 (d, 3H, $\text{CH}(\text{CH}_3)_2$, 3J (^1H - ^1H)= 7.1 Hz) $^{13}\text{C}\{^1\text{H}\}$ NMR (CDCl_3 , 125.9 MHz, 301.2 K) δ 169.9 (Q), 165.1 (Q), 157.1 (Q, C-Br), 141.7 (Q), 132.1 (CH), 130.0 (2 x CH), 129.7 (CH), 129.3 (CH), 127.8 (CH), 125.4 (CH), 125.4 (CH), 123.3 (CH), 122.2 (Q), 101.0 (Q), 94.8 (methine CH), 87.1 (CH), 84.6 (CH), 84.4 (CH), 79.4 (CH), 30.5 ($\text{CH}(\text{CH}_3)_2$), 24.7 (aliphatic CH_3), 23.3 ($\text{CH}(\text{CH}_3)_2$), 21.0 ($\text{CH}(\text{CH}_3)_2$), 18.4 (methyl CH_3) Analysis Calculated for $\text{C}_{26}\text{H}_{27}\text{BrClINORu}$: C 53.30, H 4.64, N 2.39% Analysis Found for $\text{C}_{26}\text{H}_{27}\text{BrClINORu}$: C 52.90, H 4.60, N 2.35% ES MS (+): m/z 522.03 [M^+]-Cl (79Br)

Complex 8 (0.19 g, 0.32 mmol, 66%)

^1H NMR (CDCl_3 , 300 MHz, 300 K) δ 7.76-7.70(m, 3H, 3 x CH), 7.49-7.44 (m, 3H, 3 x CH), 7.42 (br. d, 1H, CH , 3J (^1H - ^1H)= 7.6 Hz), 7.23 (a. br. t, 1H, CH , 3J (^1H - ^1H)= 7.4 Hz), 7.09 (br. d, 1H, CH , 3J (^1H - ^1H)= 6.4 Hz), 5.39 (s, 1H, methine CH), 5.35 (br. d, 1H, CH , 3J (^1H - ^1H)= 6.2 Hz), 5.16 (br. d, 1H, CH , 3J (^1H - ^1H)= 6.2 Hz), 5.07 (br. d, 1H, CH , 3J (^1H - ^1H)= 5.3 Hz), 3.68 (br. d, 1H, CH , 3J (^1H - ^1H)= 5.7 Hz), 2.66 (br. sept, 1H, $\text{CH}(\text{CH}_3)_2$, 3J (^1H - ^1H)= 6.9 Hz), 2.02 (s, 3H, methyl CH_3), 1.79 (s, 3H, aliphatic CH_3), 1.20 (a. t, 6H, $\text{CH}(\text{CH}_3)_2$, 3J (^1H - ^1H)= 6.3 Hz) $^{13}\text{C}\{^1\text{H}\}$ NMR (CDCl_3 , 75 MHz, 300 K) δ 164.9 (Q), 157.2 (Q), 138.7 (Q, C-Br), 135.2 (Q), 130.9 (2 x CH), 129.6 (CH), 128.5 (2 x CH), 127.8 (CH), 126.0 (CH), 125.5 (CH), 123.3 (CH), 100.9 (Q), 96.2 (Q), 94.4 (methine CH), 87.1 (CH), 84.6 (CH), 84.5 (CH), 79.4 (CH), 30.5 ($\text{CH}(\text{CH}_3)_2$), 24.7 (aliphatic CH_3), 23.3 ($\text{CH}(\text{CH}_3)_2$), 20.9 ($\text{CH}(\text{CH}_3)_2$), 18.4 (methyl CH_3) Analysis Calculated for $\text{C}_{26}\text{H}_{27}\text{BrClINORu}$: C 53.30, H 4.64, N 2.39% Analysis Found for $\text{C}_{26}\text{H}_{27}\text{BrClINORu}$: C 53.20, H 4.65, N 2.30% ES MS (+): m/z 552.03 [M^+]-Cl (79Br)

Complex 9 (0.16 g, 0.25 mmol, 62%)

^1H NMR (CDCl_3 , 300 MHz, 300 K) δ 7.74 (d, 2H, 2 x CH , 3J (^1H - ^1H)= 8.3 Hz), 7.49-7.44 (m, 3H, 3 x CH), 7.42 (br. d, 1H, CH , 3J (^1H - ^1H)= 7.6 Hz), 7.23 (a. br. t, 1H, CH , 3J (^1H - ^1H)= 7.4 Hz), 7.09 (br. d, 1H, CH , 3J (^1H - ^1H)= 6.4 Hz), 5.39 (s, 1H, methine CH), 5.35 (br. d, 1H, CH , 3J (^1H - ^1H)= 6.2 Hz), 5.16 (br. d, 1H, CH , 3J (^1H - ^1H)= 6.2 Hz), 5.07 (br. d, 1H, CH , 3J (^1H - ^1H)= 5.3 Hz), 3.68 (br. d, 1H, CH , 3J (^1H - ^1H)= 5.7 Hz), 2.66 (br. sept, 1H, $\text{CH}(\text{CH}_3)_2$, 3J (^1H - ^1H)= 6.9 Hz), 2.02 (s, 3H, methyl CH_3), 1.79 (s, 3H, aliphatic CH_3), 1.20 (a. t, 6H, $\text{CH}(\text{CH}_3)_2$, 3J (^1H - ^1H)= 6.3 Hz) $^{13}\text{C}\{^1\text{H}\}$ NMR (CDCl_3 , 75 MHz, 300 K) δ 165.0 (Q), 157.2 (Q), 137.0 (Q, C-Cl), 135.2 (Q), 130.9 (2 x CH), 129.7 (CH), 128.7 (2 x CH), 127.8 (CH), 126.0 (CH), 125.5 (CH), 123.3 (CH), 100.9 (Q), 95.7 (Q), 94.5 (methine CH), 87.1 (CH), 84.7 (CH), 84.5 (CH), 79.5 (CH), 30.5 ($\text{CH}(\text{CH}_3)_2$), 24.7 (aliphatic CH_3), 23.4 ($\text{CH}(\text{CH}_3)_2$), 21.0 ($\text{CH}(\text{CH}_3)_2$), 18.4 (methyl CH_3) Analysis Calculated for $\text{C}_{26}\text{H}_{27}\text{ClINORu}$: C 49.34, H 4.30, N 2.21% Analysis Found for $\text{C}_{26}\text{H}_{27}\text{ClINORu}$: C 48.80, H 4.30, N 2.20% ES MS (+): m/z 632.85 [M^+]

Complex 10 (0.16 g, 0.29 mmol, 68%)

^1H NMR (CDCl_3 , 500.57 MHz, 300.7 K) δ 7.82 (br. d, 2H, CH , 3J (^1H - ^1H)= 8.7 Hz), 7.76 (br. d, 1H, CH , 3J (^1H - ^1H)= 8.2 Hz), 7.42 (br. t, 2H, CH , 3J (^1H - ^1H)= 7.6 Hz), 7.25-7.20 (m, 1H, CH), 7.10 (br. d, 1H, CH , 3J (^1H - ^1H)= 7.4 Hz), 6.84 (br. d, 2H, CH , 3J (^1H - ^1H)= 8.7 Hz), 5.39 (s, 1H, methine CH), 5.34 (br. d, 1H, CH , 3J (^1H - ^1H)= 5.0 Hz), 5.16 (br. d, 1H, CH , 3J (^1H - ^1H)= 6.0 Hz), 5.05 (br. d, 1H, CH , 3J (^1H - ^1H)= 5.0 Hz), 4.07 (q, 2H, ethoxy CH_2 , 3J (^1H - ^1H)= 6.9 Hz), 3.69 (br. d, 1H, CH , 3J (^1H - ^1H)= 5.0 Hz), 2.68 (br. sept, 1H, $\text{CH}(\text{CH}_3)_2$, 3J (^1H - ^1H)= 7.4 Hz), 2.03 (s, 3H, methyl CH_3), 1.78 (s, 3H, aliphatic CH_3), 1.43 (t, 3H, ethoxy CH_3 , 3J (^1H - ^1H)= 6.9 Hz), 1.24-1.16 (br. t, 6H, $\text{CH}(\text{CH}_3)_2$, 3J (^1H - ^1H)= 6.9 Hz) $^{13}\text{C}\{^1\text{H}\}$ NMR (CDCl_3 , 125.5 MHz, 300.7 K) δ 171.4 (Q), 164.3 (Q), 160.2 (Q), 157.4 (Q), 131.0 (Q), 128.5 (2 x CH), 127.7 (2 x CH), 126.3 (CH), 125.3 (CH), 123.7 (CH), 113.6 (2 x CH), 100.7 (Q), 96.1 (Q), 93.5 (methine CH), 87.1 (CH), 84.6 (CH), 84.4 (CH), 79.4 (CH), 63.4 (ethoxy CH_2), 30.5 ($\text{CH}(\text{CH}_3)_2$), 24.7 (aliphatic CH_3), 23.4 ($\text{CH}(\text{CH}_3)_2$), 21.0 ($\text{CH}(\text{CH}_3)_2$), 18.4 (methyl CH_3), 14.8 (ethoxy CH_3) Analysis Calculated for $\text{C}_{28}\text{H}_{32}\text{ClINORu}$: C 61.03, H 5.85, N 2.54, Cl 6.43% Analysis Found for $\text{C}_{28}\text{H}_{32}\text{ClINORu}$: C 59.65, H 5.85, N 2.55, Cl 6.43% ES MS (+): m/z 516.15 [M^+]-Cl

Complex 11 (0.06 g, 0.12 mmol, 62%)

^1H NMR (CDCl_3 , 300 MHz, 300 K) δ 7.76 (br. d, 2H, CH , 3J (^1H - ^1H)= 8.3 Hz), 7.42 (br. t, 2H, CH , 3J (^1H - ^1H)= 7.7 Hz), 7.25-7.20 (m, 2H, CH), 7.14 (br. d, 2H, CH , 3J (^1H - ^1H)= 7.9 Hz), 7.09 (br. d, 1H, CH , 3J (^1H - ^1H)= 7.2 Hz), 5.42 (s, 1H, methine CH), 5.35 (br. d, 1H, CH , 3J (^1H - ^1H)= 6.0 Hz), 5.17 (br. d, 1H, CH , 3J (^1H - ^1H)= 6.0 Hz), 5.06 (br. d, 1H, CH , 3J (^1H - ^1H)= 5.7 Hz), 3.69 (br. d, 1H, CH , 3J (^1H - ^1H)= 5.7 Hz), 2.68 (br. sept, 1H, $\text{CH}(\text{CH}_3)_2$, 3J (^1H - ^1H)= 6.9 Hz), 2.37 (s, 3H, methyl CH_3), 2.03 (s, 3H, methyl CH_3), 1.79 (s, 3H, aliphatic CH_3), 1.24-1.16 (m, 6H, $\text{CH}(\text{CH}_3)_2$) $^{13}\text{C}\{^1\text{H}\}$ NMR (CDCl_3 , 75 MHz, 300 K) δ 171.7 (Q), 164.5 (Q), 157.4 (Q), 139.4 (Q), 136.8 (Q), 128.5 (2 x CH), 127.6 (2 x CH), 126.9 (CH), 125.3 (CH), 123.5 (CH), 100.7 (Q), 96.2 (Q), 94.0 (methine CH), 87.2 (CH), 84.6 (CH), 84.4 (CH), 79.4 (CH), 30.4 ($\text{CH}(\text{CH}_3)_2$), 24.7 (aliphatic CH_3), 23.4 ($\text{CH}(\text{CH}_3)_2$), 21.4 (methyl CH_3), 20.9 ($\text{CH}(\text{CH}_3)_2$), 18.4 (methyl CH_3) Analysis Calculated for $\text{C}_{27}\text{H}_{30}\text{ClINORu}$: C 62.24, H 5.80, N 2.69, Cl 6.80% Analysis Found for $\text{C}_{27}\text{H}_{30}\text{ClINORu}$: C 62.10, H 5.85, N 2.65, Cl 6.85% ES MS (+): m/z 486.14 [M^+]-Cl

Complex 12 (0.10 g, 0.17 mmol, 61%)

¹H NMR (CDCl₃, 300 MHz, 300 K) δ 7.85-7.78 (m, 3H, 3 x CH), 7.53-7.36 (m, 9H, 9 x CH), 5.60 (s, 1H, methine CH), 5.56 (br. d, 1H, CH, ³J (H-H) = 6.2 Hz), 5.49 (br. d, 1H, CH, ³J (H-H) = 5.5 Hz), 5.27 (br. d, 2H, CH, ³J (H-H) = 5.7 Hz), 3.00-2.90 (br. q, 1H, CH(CH₃)₂), 2.13 (s, 3H, methyl CH₃), 1.57 (s, 3H, aliphatic CH₃), 1.35 (dd, 6H, CHC(CH₃)₂, ³J (H-H) = 6.9 Hz and ³J (H-H) = 3.9 Hz) ¹³C{¹H} NMR (CDCl₃, 75 MHz, 300 K) δ 162.4 (Q), 154.3 (Q), 148.3 (Q), 133.7 (Q), 126.7 (Q), 125.4 (Q), 129.8 (CH), 127.8 (CH), 126.4 (CH), 126.0 (CH), 125.0 (CH), 124.6 (CH), 100.8 (Q), 99.8 (methine CH), 97.5 (Q), 84.3 (CH), 82.5 (CH), 79.1 (CH), 79.0 (CH), 30.7 (CH(CH₃)), 27.9 (aliphatic CH₃), 22.4 (CH(CH₃)₂), 22.3 (CH(CH₃)₂), 17.9 (methyl CH₃) Analysis Calculated for C₃₀H₃₀ClNO: C 64.68, H 5.43, N 2.51, Cl 6.36% Analysis Found for C₃₀H₃₀ClNO: C 61.70, H 5.35, N 1.55, Cl 7.30% ES MS (+): m/z 522.1 [M⁺]-Cl

Complex 13 (0.18 g, 0.32 mmol, 62%)

¹H NMR (CDCl₃, 300.13 MHz, 300.0 K) δ 7.88-7.81 (m, 2H, CH), 7.65 (ddd, 1H, CH, ³J (H-¹⁹F) = 9.3 Hz, ⁴J (H-¹⁹F) = 6.2 Hz and ⁴J (H-H) = 3.2 Hz), 7.18 (td, 1H, CH, ³J (H-¹⁹F) = 9.1 Hz and ³J (H-H) = 4.8 Hz), 7.06-6.97 (m, 2H, CH), 6.93 (ddt, 1H, CH, ³J (H-¹⁹F) = 9.1 Hz, ³J (H-H) = 7.2 Hz and ⁴J (H-¹⁹F) = 3.5 Hz), 5.43 (s, 1H, methine CH), 5.41 (br. d, 1H, CH, ³J (H-H) = 5.7 Hz), 5.24 (br. d, 1H, CH, ³J (H-H) = 5.7 Hz), 5.18 (br. d, 1H, CH, ³J (H-H) = 6.2 Hz), 3.86 (br. d, 1H, CH, ³J (H-H) = 5.5 Hz), 2.65 (br. sept, 1H, CH(CH₃)₂, ³J (H-H) = 7.0 Hz), 2.05 (s, 3H, methyl CH₃), 1.82 (br. d, 3H, aliphatic CH₃, ³J (H-¹⁹F) = 0.8 Hz), 1.18 (dd (vt), 6H, CH(CH₃)₂, ³J (H-H) = 7.3 Hz) ¹³C{¹H} NMR (CDCl₃, 75.5 MHz, 300.1 K) δ 166.1 (Q), 163.8 (d, Q, C-F, ¹J (C-¹⁹F) = 247.2 Hz), 161.4 (Q), 155.0 (d, Q, C-F, ¹J (C-¹⁹F) = 213.9 Hz), 152.6 (d, Q, C-F, ¹J (C-¹⁹F) = 225.0 Hz), 135.4 (Q), 131.3 (d, Q, ²J (C-¹⁹F) = 119.9 Hz) 128.9 (2 x CH, ³J (C-¹⁹F) = 8.7 Hz), 115.8 (d, CH, ²J (C-¹⁹F) = 23.5 Hz), 115.6 (d, CH, ²J (C-¹⁹F) = 23.5 Hz), 114.7 (2 x CH, ²J (C-¹⁹F) = 22.3 Hz), 113.3 (d, CH, ²J (C-¹⁹F) = 16.1 Hz), 101.1 (Q), 96.1 (Q), 94.2 (methine CH), 86.9 (CH), 84.9 (CH), 84.3 (CH), 78.5 (CH), 30.6 (CH(CH₃)₂), 23.9 (CH(CH₃)₂), 23.2 (CH(CH₃)₂), 20.7 (aliphatic CH₃), 18.3 (methyl CH₃) Analysis Calculated for C₂₆H₂₅ClF₃NORu: C 55.66, H 4.49, N 2.50% Analysis Found for C₂₆H₂₅ClF₃NORu: C 55.45, H 4.50, N 2.45% ES MS (+): m/z 526.09 [M⁺]-Cl

Complex 14 (0.08 g, 0.21 mmol, 57%)

Complex 14 was synthesised according to the previous ruthenium complex preparation, with addition of 2 equivalents of diphenyl-β-ketoiminate ligand. ¹H NMR (CDCl₃, 300 MHz, 300.0 K) δ 7.90-7.85 (m, 2H, CH), 7.61-7.56 (m, 2H, CH), 7.45-7.30 (m, 2H, CH), 5.72 (d, 1H, NH, ⁴J (H-H) = 2.3 Hz), 5.45 (br. s, 2H, CH), 5.21 (m, 2H, CH), 2.85 (br. sept, 1H, CH(CH₃)₂, ³J (H-H) = 7.0 Hz), 2.30 (s, 3H, methyl CH₃), 1.32 (br. d, 6H, CH(CH₃)₂, ³J (H-H) = 6.8 Hz) ¹³C{¹H} NMR (CDCl₃, 75 MHz, 300.0 K) δ 210.3 (Q), 206.4 (Q), 174.5 (Q), 159.3 (Q), 129.7 (CH), 128.7 (CH), 127.8 (CH), 126.9 (CH), 126.2 (CH), 100.9 (Q), 99.8 (Q), 99.3 (methine CH), 91.8 (CH), 84.9 (CH), 30.7 (CH(CH₃)₂), 25.2 (2 x CH(CH₃)₂), 18.3 (methyl CH₃) Analysis Calculated for C₂₀H₂₄ClNO: C 60.91, H 5.32, N 2.84, Cl 7.19% Analysis Found for C₂₀H₂₄ClNO: C 60.90, H 5.30, N 3.10, Cl 7.40% ES MS (+): m/z 456.33 [M⁺]-Cl

Complex 17 (0.04 g, 0.06 mmol, 46%)

Complex 17 was synthesised according to the previous ruthenium complex preparation, with addition of 2 equivalents of NH-β-ketoiminate ligand.

¹H NMR (300 MHz, CDCl₃, 300 K) δ 7.86-7.83 (m, 2H, CH), 7.31 (ddd, 3H, CH, ³J (H-H) = 19.21 Hz, 11.5 Hz and 7.6 Hz), 5.38 (d, 1H, methine CH, ³J (H-H) = 2.1 Hz), 2.09 (s, 3H, aliphatic CH₃), 1.68 (br. s, 15H, Cp * methyl CCH₃) ¹³C{¹H} NMR (125 MHz, CDCl₃, 300 K) δ 170.8 (Q), 163.1 (Q), 139.8 (Q), 129.3 (CH), 128.0 (2 x CH), 126.7 (2 x CH), 94.0 (methine CH), 84.7 (Q, Cp* C(CH₃)₃), 28.6 (aliphatic CH₃), 8.7 (Cp * methyl, C(CH₃)) Analysis Calculated for C₂₀H₂₅ClIrNO: C 45.9, H 4.8, N 2.6 % Analysis Found for C₂₀H₂₅ClIrNO: C 45.9, H 4.8, N 2.6 %

Complex 18 (0.07 g, 0.13 mmol, 58%)

Complex 18 was synthesised by addition of [Cp*IrCl₂]₂ (1 eq), a 3-fluoro-β-diketonate ligand (2 eq) and Et₃N (2 eq). All were stirred in dichloromethane (30 mL) at room temperature overnight. The solvent removed under reduced pressure and the crude product recrystallised using slow evaporation from a methanolic solution.

¹H NMR (CDCl₃, 300 MHz, 299.2 K) δ 7.66-7.61 (m, 1H, CH), 7.61-7.54 (m, 1H, CH), 7.35-7.28 (m, 1H, CH), 7.19-7.10 (m, 1H, CH), 5.85 (s, 1H, methine CH), 2.08 (s, 3H, CH₃), 1.66 (br. s, 15H, Cp* methyl C(CH₃)₃) ¹³C{¹H} NMR (CDCl₃, 75 MHz, 300 K) δ 187.3 (Q), 175.5 (Q), 162.7 (d, Q, C-F, ¹J (C-¹⁹F) = 243.5 Hz), 141.1 (Q), 129.6 (d, CH, ³J (C-¹⁹F) = 8.7 Hz), 122.6 (d, CH, ⁴J (C-¹⁹F) = 2.5 Hz), 117.5 (d, CH, ²J (C-¹⁹F) = 21.0 Hz), 113.9 (d, CH, ²J (C-¹⁹F) = 23.5 Hz), 97.3 (methine CH), 83.7 (Q, Cp* C(CH₃)₃), 28.2 (aliphatic CH₃), 8.7 (Cp* methyl C(CH₃)) Analysis Calculated for C₂₀H₂₃ClF₃IrO₂: C 44.31, H 4.28 % Analysis Found for C₂₀H₂₃ClF₃IrO₂: C 44.55, H, 4.20,% ES MS (+): m/z 507.0 [MH⁺]-Cl.

Cell Line Chemosensitivity Studies

In vitro chemosensitivity tests were performed at the Institute of Cancer Therapeutics, Bradford, against MCF-7 (human breast adenocarcinoma), HT-29 (human colon adenocarcinoma), A2780 (human ovarian carcinoma) and A2780cis (cisplatin resistant A2780 cells) cell lines. Growth inhibitory effects were also tested against ARPE-19 cells. ARPE-19 are a human retinal epithelial non-cancer cell line that was obtained from the American Type Culture Collection. Cancer cell lines were routinely maintained as monolayer cultures in appropriate medium (RPMI 1640 supplemented with 10% foetal calf serum, sodium pyruvate (1 mM) and L-glutamine (2 mM) AREP-19 cells were cultured in DMEM-F12 medium containing 10% foetal calf serum. For chemosensitivity studies, cells were incubated in 96-well plates at a concentration of 2 × 10³ cells per well and the plates were incubated for 24 hours at 37 °C in an atmosphere of 5% CO₂ prior to drug exposure. Complexes or cisplatin were each dissolved in dimethylsulfoxide to provide stock solutions that were diluted to provide a range of final concentrations. Drug solutions were added to cells (the final DMSO concentrations was less than 0.1% (v/v) in all cases) and incubated for 5 days at 37 °C in an atmosphere of 5% CO₂. 3-(4,5-dimethylthiazol-2-yl)-2,5-diphenyltetrazolium bromide (MTT) (20 μL, 5 mg mL⁻¹) was added to each well and incubated for 3 hours at 37 °C in an atmosphere of 5% CO₂. All solutions were then removed *via* pipette and 150 μL

of dimethylsulfoxide added to each well in order to dissolve the purple formazan crystals. A Thermo Scientific Multiskan EX microplate photometer was used to measure the absorbance of each well at 540 nm. Lanes containing medium only and 100% cells were used as blanks for the spectrophotometer and 100% cell survival respectively. Cell survival was determined as the absorbance of treated cells divided by the absorbance of controls and expressed as a percentage. The IC_{50} values were determined from plots of % survival against drug concentration. Each experiment was repeated three times and a mean value obtained and stated as IC_{50} (μM) \pm SD. To quantify the response of tumour cells compared to normal cells, IC_{50} values were expressed as the ratio of IC_{50} in ARPE-19 cells divided by the IC_{50} for individual tumour cells evaluated. A ratio of greater than 1 indicates selectivity towards cancer cells. IC_{50} values (μM) and the standard deviations (SD) after a minimum of three repeats are presented in **Figure S2** (see SI)

Influence of Hypoxia

The hypoxia assay was conducted according to the protocol stated previously for normoxic conditions. However, the incubation period, the addition of the drug dilutions and the addition of the MTT solution were carried out inside a Don Whitley Scientific H35 Hypoxystation which was set at 1.0 or 0.1% O_2 . Cisplatin was tested as a comparison and a well-known hypoxic sensitive compound tirapazimine (TPZ) was tested as a positive control. These results are presented in **Table S3a** and **S3b** (see SI).

Inhibition of thioredoxin reductase activity

Thioredoxin reductase sourced from rat liver was obtained from Sigma Aldrich. It is a buffered aqueous glycerol solution, ≥ 100 units/ mg protein. Solution in 50 mM Tris-HCl, pH 7.5, 300 mM NaCl, 1 mM EDTA, and 10% glycerol. The rate of change of UV-vis absorbance was measured at 412 nm over 1 min to give the reaction velocity. The experiment was carried out using just the enzyme to get the control (no inhibitor) reaction velocity and then varying dilutions of the test compound were added up to a maximum of 10 μM . The reaction velocity in the presence of inhibitor was normalised relative to the control to generate % activity and plots of % activity versus concentration were constructed to obtain IC_{50} values (concentration that inhibited 50% of enzyme activity) For full experimental and IC_{50} values cf. **Figure S3** (see SI).

Induction of Cancer Cell Death by Apoptosis

Cells were incubated in T-25 flasks and diluted to concentrations of 2.5×10^4 cells/flask (0.5×10^4 cells/ mL) using complete RMPI 1640 medium. These were incubated for 24 hours at 37°C in an atmosphere of 5.0% CO_2 . Complexes were dissolved in dimethylsulfoxide and then further diluted with RMPI 1640 to obtained concentrations ranging from 20-0 μM . The cells were then incubated with the varying concentrations of complex for 48 hours, media/drug solutions were removed and flasks were washed with PBS (5 mL), adding all washings to a centrifuge tube. Trypsin (1 mL/flask) was added to each flask and then incubated for 5 minutes until a single cell suspension was obtained. The trypsin was then neutralised with medium (5 mL) and the whole contents of the flask transferred to the same centrifuge tube. The tube was centrifuged at 1000 rcf for 3-5 minutes, the supernatant removed and the pellet re-

suspended in PBS (1 mL). The 1 mL was transferred to an Eppendorf and centrifuged at 1500 rpm for 5 minutes. The supernatant was removed and the pellet re-suspended in 16 μL PI, 16 μL AmV and 800 μL buffer solution (100 μL). The Eppendorfs were incubated at room temperature for 10 minutes and kept in suspension; and then transferred to FACS tubes for analysis. Samples were run using flow cytometry and parameters adjusted depending on the sample tested. A cell count of 10,000 was necessary to conduct this experiment and gave results of PI versus Annex V, each quadrant was analysed manually and a percentage taken from each quadrant of the plot, and values are presented in **Table S8** (see SI).

Analysis of cellular DNA damage by the comet assay

Slides containing a layer of agarose were prepared in advance, using 1% normal melting point agarose (500 mg) in PBS (50 mL). The cells were diluted with complete RMPI 1640 to a concentration of 1×10^6 cells/ mL, 2 mL of the cell suspension was placed in each well of a 6-well plate. The cells were incubated for 24 hours at 37°C in a 5.0% CO_2 atmosphere. Drug samples were prepared in the range 20-0 μM , the medium was removed from the wells, and 2 mL of drug sample added to each well. The plate was then incubated again for 24 hours in the drug solutions, at 37°C in a 5.0% CO_2 atmosphere. The drug samples were removed and added to centrifuge tubes, the wells each washed with PBS (1 mL), which was also placed into the centrifuge tube. The wells were then trypsinised (1 mL) for 5 minutes and then neutralised with complete medium (1 mL), these were all added to the centrifuge tube and centrifuged at 1500 rpm for 3 minutes. The supernatant was removed and the pellet re-suspended in complete medium containing 10% DMSO (no not use DMSO with single strand assay). The tubes were wrapped in several sheets of tissue and stored at -80°C until required for the assay. When conducting the cross-linking assay, the same protocol is followed with an additional step of exposing the cells to 10% H_2O_2 for 20 minutes before harvesting the cells. For reagents, conditions and graphically analysis see **Figure S4-6** (SI)

Supporting Information: Crystallographic data and selected bond lengths and angles for ligands **L3-6**, **8** and **11**, and complexes **2**, **4-14**, **17** and **18**. Additional assays on hydrophobicity and hydrolysis. IC_{50} figures and tables for normoxic (HT-29, MCF-7, A2780, A2780cis and ARPE-19) and hypoxic assays (HT-29). Chemicals, experimental and data curves for thioredoxin reductase assay. Cell viability (%) for apoptosis studies (HT-29 and A2780), chemicals and experimental. Comet assay chemicals, experimental and bar-charts, with selected microscope images. This material is available free of charge via the Internet at <http://pubs.acs.org>.

AUTHOR INFORMATION

Corresponding Author

* Dr Patrick C. McGowan, School of Chemistry, University of Leeds, Leeds, UK, LS2 9JT. Email: p.c.mcgowan@leeds.ac.uk, Tel: +44(0)113 3436404

Author Contributions

The manuscript was written through contributions of all authors. All authors have given approval to the final version of the manuscript. ‡These authors contributed equally.

ACKNOWLEDGMENT

We would like to thank the EPSRC for funding and all the technical staff at the University of Leeds for help with NMR (Mr Simon Barrett), mass spectrometry (Ms. Tanya Marinko-Covell) and microanalysis (Mr. Ian Blakeley).

ABBREVIATIONS

A2780, human ovarian carcinoma, A2780cis, cisplatin resistant human ovarian carcinoma, Cp*, pentamethylcyclopentadienyl, HIF-1, hypoxia-inducible factor-1, HT-29, human colon carcinoma, IC₅₀, 50% inhibitory concentration, MCF-7, human breast carcinoma, NMR, Nuclear Magnetic Resonance, Trx-R, thioredoxin reductase, DSB, Double Strand Breakage, SSB, Single Strand Breakage.

REFERENCES

1. Suss-Fink, G. Arene ruthenium complexes as anticancer agents. *Dalton Trans.* **2010**, 39, 1673-1688.
2. Reedijk, J. Metal-ligand exchange kinetics in platinum and ruthenium complexes. Significance for effectiveness as anticancer drugs. *Platinum Met. Rev.*, **2008**, 52, 2-11.
3. Allardyce, C. S.; Dyson P. J. Ruthenium in medicine: current clinical uses and future prospects. *Platinum Met. Rev.* **2001**, 45, 62-69.
4. Clarke, M. J. Ruthenium metallopharmaceuticals. *Coord. Chem. Rev.* **2003**, 236, 209-233.
5. Morris, R. E.; Aird, R. E.; P. d. S. Murdoch, P. d. S.; Chen, H.; Cummings, J.; Hughes, N. D.; Parsons, S.; Parkin, A.; Boyd, G.; Jodrell, D. I.; Sadler, P. J. Inhibition of Cancer Cell Growth by Ruthenium(II) Arene Complexes. *J. Med. Chem.*, **2001**, 44, 3616-3621.
6. Aird, R. E.; Cummings, J.; Ritchie, A. A.; Muir, M.; Morris, R. E.; Chen H.; Sadler, P.J. In vitro and in vivo activity and cross resistance profiles of novel ruthenium (II) organometallic arene complexes in human ovarian cancer. *Brit. J. Cancer*, **2002**, 86, 1652-1657
7. Habtemariam, A.; Melchart, M.; Fernandez, R.; Parsons, S.; Oswald, I. D. H.; Parkin, A.; Fabbiani, F. P. A.; Davidson, J. E.; Dawson, A.; Aird, R. E.; Jodrell D. L.; Sadler, P. J. Structure-activity relationships for cytotoxic ruthenium(II) arene complexes containing N,N-, N,O-, and O,O-chelating ligands. *J. Med. Chem.*, **2006**, 49, 6858-6868.
8. Fernandez, R.; Melchart, M.; Habtemariam, A.; Parsons, S.; Sadler, P. J. Use of chelating ligands to tune the reactive site of half-sandwich ruthenium(II) arene anticancer complexes. *Chem. Eur. J.* **2004**, 10, 5173-5179.
9. Chou, M. H.; Szalda, D. J.; Creutz, C.; Sutin, N. Reactivity and coordination chemistry of aromatic carboxamide RC(O)NH₂ and carboxylate ligands: properties of pentaammine ruthenium(II) and -(III) complexes. *Inorg. Chem.* **1994**, 33, 1674-1684.
10. Ford, P. C.; Rudd, D. P.; Gaunder, R.; Taube, H. Synthesis and properties of pentaamminepyridineruthenium(II) and relate pentaammineruthenium complexes of aromatic nitrogen heterocycles. *J. Am. Chem. Soc.* **1968**, 90, 1187-1194.
11. Singh, A. K.; Balamurugan, V.; Mukherjee, R. Synthesis and characterization of low-spin and cation radical complexes of ruthenium(III) of a tridentate pyridine bis-amide ligand. *Inorg. Chem.* **2003**, 42, 6497-6502
12. Rijt, S. H. van.; Hebden, A. J., Amaresekera, T.; Deeth, R. J.; Clarkson, G. J.; Parsons, P.; McGowan, P. C.; Sadler, P. J. Amide Linkage Isomerism As an Activity Switch for Organometallic Osmium and Ruthenium Anticancer Complexes. *J. Med. Chem.* **2009**, 52, 7753-7764.
13. Camm, K. D.; El-Sokkary, A.; Gott, A. L.; Stockley, P. G.; Belyaeva, T.; McGowan, P. C. Synthesis, molecular structure and evaluation of new organometallic ruthenium anticancer agents. *Dalton Trans.* **2009**, 10914-10925.
14. Lucas, S. J., Lord, R. M., Wilson, R. L., Phillips, R. M., Sridharana, V. and McGowan, P.C. Synthesis of iridium and ruthenium complexes with (N,N), (N,O) and (O,O) coordinating bidentate ligands as potential anti-cancer agents. *Dalton Trans.* **2012**, 41, 13800-13802.
15. Rohwer, N.; Cramer, T. Hypoxia-mediated drug resistance: novel insights on the functional interaction of HIFs and cell death pathways. *Drug Resist Updat* **2011**, 14, 191-201.
16. Brown, J.M. Tumor microenvironment and the response to anticancer therapy. *Cancer Biol Ther* **2002**, 1, 453-458.
17. Ahmadi M, Ahmadihosseini Z, Allison SJ, Begum S, Rockley K, Sadiq M, Chintamaneni S, Lokwani R, Hughes N, Phillips RM. Hypoxia modulates the activity of a series of clinically approved tyrosine kinase inhibitors. *Br. J. Pharmacol.* **2014**, 171: 224-36.
18. Roshchupkina, G. I., Gatilov, Y. V., Rybalova, T. V. and Reznikov, V. A. Reactions of 1,3-Diaryl-2-chloropropane-1,3-diones with Nucleophiles - Cyanide-Induced Retro-Claisen-Claisen Condensation. *Eur. J. Org. Chem.*, **2004**, 2004, 765-73.
19. Levine, R.; Sneed, J. K. The Relative Reactivities of the Isomeric Methyl Pyridinecarboxylates in the Acylation of Certain Ketones. The Synthesis of β -Diketones Containing Pyridine Rings. *J. Am. Chem. Soc.* **1951**, 73, 5614-5616.
20. Hollick, J. J.; Golding, B. T.; Hardcastle, I. R.; Martin, N.; Richardson, C.; Rigoreau, L. J. M.; Smith, G. C. M.; Griffin, R. J. 2,6-Disubstituted pyran-4-one and thiopyran-4-one inhibitors of DNA-Dependent protein kinase (DNA-PK). *Bioorg. Med. Chem. Lett.* **2003**, 13, 3083-3086.
21. Tang, L. -M.; Duan, Y. -Q.; Li, X. -F.; Li, Y. -S. Syntheses, structure and ethylene polymerization behavior of β -diiminato titanium complexes. *J. Organomet. Chem.*, **2006**, 691, 2023-2030.
22. Pettinari, R.; Pettinari, C.; Marchetti, F.; Clavel, C. M.; Scopelliti, R.; Dyson, P. J. Cytotoxicity of Ruthenium-Arene Complexes Containing β -Ketoamine Ligands. *Organometallics*. **2012**, 32, 309-316.
23. Semenza, G. L. Hydroxylation of HIF-1: Oxygen Sensing at the Molecular Level. *Physiology*, **2004**, 19, 176-182.
24. Krishnamachary, B.; Berg-Dixon, S.; Kelly, B.; Agani, F.; Feldser, D.; Ferreira, G.; Iyer, N.; LaRusch, J.; Pak, B.; Taghavi, P.; Semenza, G. L. Regulation of colon carcinoma cell invasion by hypoxia-inducible factor 1. *Cancer Res.* **2003**, 63, 1138-1142.
25. Pennacchietti, S.; Michieli, P.; Galluzzo, M.; Mazzone, M.; Giordano, S.; Comoglio, P. M. *Cancer Cell*, **2003**, 3, 347-361.
26. Semenza, G. L. Involvement of hypoxia-inducible factor 1 in human cancer. *Internal Medicine*. **2001**, 41, 79-83.
27. Wykoff, C. C.; Pugh, C. W.; Maxwell, P. H.; Harris, A. L.; Ratcliffe, p. J. Identification of novel hypoxia dependent and independent target genes of the von Hippel-Lindau (VHL) tumour suppressor by mRNA differential expression profiling. *Oncogene*, **2000**, 19, 54, 6297-6305.
28. Koch, C. J. The unusual dependence on oxygen concentration of toxicity by SR-4233 [3-amino-1,2,4-benzotriazine-1,4-dioxide]; an hypoxic cell toxin. *Cancer Res.*, **1993**, 53, 3992-3997
29. Arner, E. S.; Holmgren, A. The thioredoxin system in cancer. *Semin. Cancer Biol.* **2006**, 16, 420-426.
30. Berggren, M.; Gallegos, A.; Gasdaska, J. R.; Gasdaska, P. Y.; Warneke, J.; Powis, G. Thioredoxin and thioredoxin reductase gene expression in human tumors and cell lines, and the effects

- of serum stimulation and hypoxia. *Anticancer Res.* **1996**, *16*, 3459-3466.
31. Soini, Y.; Kahlos, K.; Näpänkangas, U.; Kaarteenaho-Wiik, R.; Säily, M.; Koistinen, P.; Pääkkö, P.; Holmgren, A.; Kinnula, V. L. Widespread expression of thioredoxin and thioredoxin reductase in non-small cell lung carcinoma. *Clin. Cancer Res.* **2001**, *7*, 1750-1757.
32. Kahlos, K.; Soini, Y.; Säily, M.; Koistinen, P.; Kakko, S.; Paakko, P.; Holmgren, A.; Kinnula, V. L., Up-regulation of thioredoxin and thioredoxin reductase in human malignant pleural mesothelioma. *Int. J. Cancer*, **2001**, *95*, 198-204.
33. Almodares, Z.; Lucas, S. J.; Crossley, B. D.; Basri, A. M.; Pask, C. M.; Hebden, A. J.; Phillips R. M.; McGowan, P. C Rhodium, Iridium, and Ruthenium Half-Sandwich Picolinamide Complexes as Anticancer Agents. *Inorg.Chem.* **2014**, *53*, 727-736.
34. Rudd, G. N.; Hartley, G. A.; Souhami, R. L. Persistence of cisplatin-induced DNA interstrand cross-linking in peripheral-blood mononuclear-cells from elderly and young individuals. *Cancer Chemot. Pharm.* **1995**, *35*, 323-326.
35. Poklar, N.; Pilch, D. S.; Lippard, S. J.; Redding, E. A.; Dunham, S. U.; Breslauer, K. J. Influence of cisplatin intrastrand crosslinking on the conformation, thermal stability, and energetics of a 20-mer DNA duplex. *Proc. Natl. Acad. Sci. U.S.A.*, **1996**, *93*, 7606-7610.
36. Kaim, W.; Schwederski, B. *Bioinorganic Chemistry: Inorganic Elements in the Chemistry of Life*, New York, 1998.
37. Cosier, J.; Glazer, A. M. A nitrogen-gas-stream cryostat for general X-ray diffraction studies. *J. Appl. Cryst.* **1986**, *19*, 105-107.
38. Otwinowski, Z.; Minor, W. in 'DENZO and SCALEPACK programs', **1995**.
39. Yarnto, England, 2014.
40. Sheldrick, G. M. A short history of SHELX. *Acta Cryst. A*, **2008**, *64*, 112-122.
41. Barbour, L. J. in 'XSeed', **1999**
42. Dolomanov, O. V.; Bourhis, L. J.; Gildea, R. J.; Howard, J. A. K.; Puschmann, H. OLEX2: a complete structure solution, refinement and analysis program. *J. Appl. Cryst.*, **2009**, *42*, 339-341.
43. Thornton-Pett, M. in 'WC-A Windows CIF Processor', **2000**.
44. Spek, A. L. Single-crystal structure validation with the program PLATON. *J. Appl. Cryst.* **2003**, *36*, 7-13
- .

